Abundance analyses of cool extreme helium stars

Gajendra Pandey,[1]★ N. Kameswara Rao,[2] David L. Lambert,[1] C. Simon Jeffery[3] and Martin Asplund[4]

[1]*Department of Astronomy, University of Texas, Austin, TX 78712-1083, USA*
[2]*Indian Institute of Astrophysics, Bangalore 560034, India*
[3]*Armagh Observatory, College Hill, Armagh BT61 9DG*
[4]*Astronomiska Observatoriet, Box 515, S-751 20 Uppsala, Sweden*

ABSTRACT

Extreme helium stars (EHes) with effective temperatures from 8000 to 13 000 K are among the coolest EHes and overlap the hotter R CrB stars in effective temperature. The cool EHes may represent an evolutionary link between the hot EHes and the R CrB stars. Abundance analyses of four cool EHes, BD+1° 4381 (FQ Aqr), LS IV −14° 109, BD −1° 3438 (NO Ser) and LS IV −1° 002 (V2244 Oph), are presented. All these stars show evidence of H- and He-burning at earlier stages of their evolution.

To test for an evolutionary connection, the chemical compositions of cool EHes are compared with those of hot EHes and R CrB stars. Relative to Fe, the N abundance of these stars is intermediate between those of hot EHes and R CrB stars. For the R CrB stars, the metallicity M derived from the mean of Si and S appears to be more consistent with the kinematics than that derived from Fe. When metallicity M derived from Si and S replaces Fe, the observed N abundances of EHes and R CrB stars fall at or below the upper limit corresponding to thorough conversion of initial C and O to N. There is an apparent difference between the composition of R CrB stars and EHes, the former having systematically higher [N/M] ratios. The material present in the atmospheres of many R CrB stars is heavily CN- and ON-cycled. Most of the EHes have only CN-cycled material in their atmospheres. There is an indication that the CN- and ON-cycled N in EHes was partially converted to Ne by α-captures. If EHes are to evolve to R CrB stars, fresh C in EHes has to be converted to N; the atmospheres of EHes have just sufficient hydrogen to raise the N abundance to the level of R CrB stars. If Ne is found to be normal in R CrB stars, the proposal that EHes evolve to R CrB stars fails. The idea that R CrB stars evolve to EHes is ruled out; the N abundance in R CrB stars has to be reduced to the level of EHes, as the C/He, which is observed to be uniform across EHes, has to be maintained. Hence the inferred [N/M], C/He and [Ne/M] ratios, and the H-abundances of these two groups indicate that the EHes and the R CrB stars may not be on the same evolutionary path.

The atmospheres of H-deficient stars probably consist of three ingredients: a residue of normal H-rich material, substantial amounts of H-poor CN(O)-cycled material, and C- (and O-) rich material from gas exposed to He-burning. This composition could be a result of final He-shell flash in a single post-AGB star (FF scenario), or a merger of two white dwarfs (DD scenario). Although the FF scenario accounts for Sakurai's object and other stars (e.g., the H-poor central stars of planetary nebulae), present theoretical calculations imply higher C/He and O/He ratios than are observed in EHes and R CrB stars. Quantitative predictions are lacking for the DD scenario.

Key words: stars: abundances – stars: AGB and post-AGB – stars: chemically peculiar – stars: evolution.

★E-mail: pandey@gandhi.as.utexas.edu

1 INTRODUCTION

The extreme helium stars (EHes) are a rare class of stars. Popper (1942) discovered the first EHe, HD 124448, and Thackeray & Wesselink (1952) the second, HD 168476. Today, about 25 are known (Jeffery 1996). Early work on the surface composition of the EHes by curve-of-growth techniques, notably by Hill (1964, 1965), concentrated on the hotter EHes whose spectra are characterized by strong lines of neutral helium, singly ionized carbon, and weak or absent Balmer lines. The first self-consistent spectroscopic analysis using hydrogen-deficient model atmospheres was performed by Schönberner & Wolf (1974) for Popper's star. Jeffery (1996) reviews modern work on abundance analyses of EHes. More recent work includes the spectral analyses of HD 144941 (Harrison & Jeffery 1997; Jeffery & Harrison 1997), LSS 3184 (Drilling, Jeffery & Heber 1998), LS IV $+6°002$ (Jeffery 1998), LSS 4357, LS II $+33°005$ and LSS 99 (Jeffery et al. 1998) and V652 Her (Jeffery, Hill & Heber 1999). Published work has emphasized the hotter EHes. Cooler EHes, stars with effective temperatures of 8000 to 13 000 K, have been largely ignored. A quartet of such EHes is analysed here.

Our stars were selected from the list provided by Jeffery et al. (1996). Three of our stars – BD $+1°4381$ (FQ Aqr), LS IV $-14°109$ and LS IV $-1°002$ (NO Ser) –were discovered by Drilling during the course of a spectroscopic survey of stars down to photographic magnitude 12.0, which had been classified as OB^+ stars in the Case-Hamburg surveys (Drilling 1979; 1980). The final member of the quartet, BD $-1°3438$ (V2244 Oph), is one of eight extreme helium stars described by Hunger (1975). Judged by effective temperature and luminosity, these cool EHes may represent an evolutionary link between the hot EHes and the R CrB stars. A major goal of our abundance analyses was to test this link using chemical compositions of the three groups of stars. Our abundance analyses are based on high-resolution optical spectra and model atmospheres.[1]

2 OBSERVATIONS

High-resolution optical spectra of the four EHes were obtained on 1996 July 25 at the W. J. McDonald Observatory 2.7-m telescope with the coudé cross-dispersed echelle spectrograph (Tull et al. 1995) at a 2-pixel resolving power ($R = \lambda/\Delta\lambda$) of 60 000. The detector was a Tektronix 2048×2048 CCD. The recorded spectrum covered the wavelength range from 3800 to 10 000 Å, but the spectral coverage was incomplete longward of about 5500 Å. A Th-Ar hollow cathode lamp was observed either just prior to or just after exposures of the programme stars to provide wavelength calibration. In order to remove the pixel-to-pixel variation in the sensitivity of the CCD, exposures were obtained of a halogen lamp. Typical exposure times of our programme stars were 30 min, and two exposures were co-added to improve the signal-to-noise ratio of the final spectrum, and to identify and eliminate cosmic rays. To cover the missing wavelength regions in the red, observations were made at a slightly different grating setting on 1996 July 26 for two of the programme stars, FQ Aqr and BD $-1°3438$. The FWHM of the Th-Ar comparison lines and the atmospheric lines present in the spectra corresponds to $6.0\,\mathrm{km\,s^{-1}}$. We have used the Image Reduction and Analysis Facility (IRAF) software packages to reduce the spectra.

[1] Preliminary analyses of FQ Aqr and LS IV $-1°$ 002 are reported by Asplund et al. (2000).
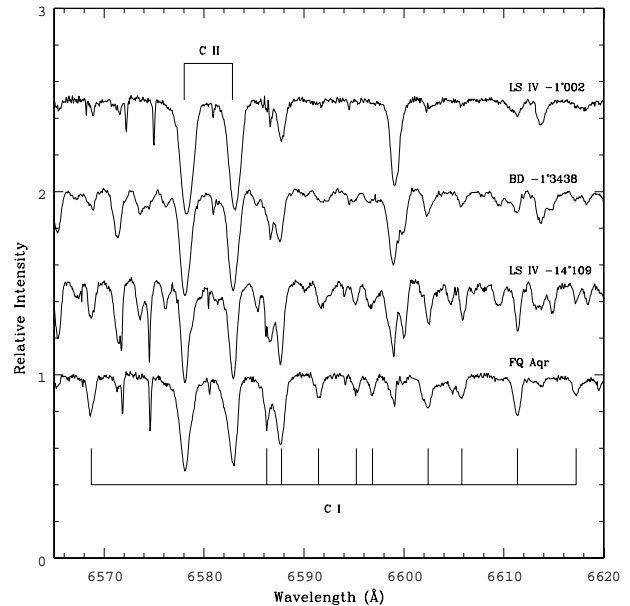
Figure 1. Region showing neutral and ionized lines of C I and C II in the spectra of cool EHes.

Lines were identified using the Revised Multiplet Table (Moore 1972), the selected Tables of Atomic Spectra (Moore 1970), the line list provided by Kurucz & Peytremann (1975), and also the investigations of Hill (1964, 1965), Lynas-Gray et al. (1981) and Heber (1983). Lines of C I, C II and He I lines were readily identified (Fig. 1). No lines of He II were found. Lines of all elements expected and observed in early A-type and late B-type normal stars were found. Lines of ionized metals of the iron group are plentiful. These lines are much stronger when compared with those observed in early A-type and late B-type normal stars, a notable feature of the spectra of cool EHes and attributable to the lower opacity in the atmosphere due to hydrogen deficiency. Our large spectral coverage enabled us to identify several important elements in one or two stages of ionization (see Fig. 1).

The photospheric radial velocities (R.V.) for the programme stars were measured using Fe II lines, and are listed in Table 1. The number of Fe II lines used is given within brackets.

3 MODEL ATMOSPHERES OF HYDROGEN-DEFICIENT STARS

Our analyses are based on model atmospheres constructed from the classical assumptions: the energy (radiation plus convection) flux is constant, and the atmosphere consists of plane-parallel layers in hydrostatic and local thermodynamic equilibrium (LTE). For the abundance analysis, a model was combined with the appropriate program to predict equivalent widths and, by iteration, to obtain the elemental abundances.

Analyses have to be self-consistent, i.e., the derived abundances should be identical to those used in constructing the model. For the cooler stars, the key quantity is the C/He ratio (Asplund et al. 1997a). Available model grids cover an adequate range in the C/He ratio. For the hot stars, helium is a controlling influence on the atmospheric structure and the C/He ratio plays a minor role.

3.1 Models for $T_{\mathrm{eff}} \leq 9500$ K

For stars with $T_{\mathrm{eff}} \leq 9500$ K, we used the Uppsala line-blanketed

Table 1. Final stellar parameters for cool extreme helium stars.

Star	T_{eff} K	$\log g$ cgs units	ξ km s^{-1}	C/He %	R.V. km s^{-1}	v_M km s^{-1}
FQ Aqr	8750 ± 250	0.75 ± 0.25	7.5 ± 0.5	0.5	16 ± 3 (59)	20
LS IV $-14°\,109$	9500 ± 250	0.90 ± 0.20	6.5 ± 0.5	1.0	5 ± 2 (47)	15
BD $-1°\,3438$	11750 ± 250	2.30 ± 0.40	10 ± 1.0	0.2	-22 ± 2 (45)	15
LS IV $-1°\,002$	12750 ± 250	1.75 ± 0.25	10 ± 1.0	0.6	-20 ± 3 (22)	20

models described by Asplund et al. (1997a). The important features of this model grid are the inclusion of line-blanketing by opacity sampling, and the use of modern values for continuous opacities from the Opacity project (Seaton et al. 1994, and references therein). Free–free opacity of He I, C I and C II (Peach 1970) have been incorporated. Electron and Rayleigh scattering opacities are included.

The grid provides models for temperatures in the range $5000 \le T_{eff} \le 9500$ K and gravities in the range $-0.5 \le \log g \le 2.0$ [cgs]. The abundances used for the standard grid are taken mainly from Lambert & Rao (1994). Models are calculated for the following values of the C/He ratio: C/He = 0.1, 0.3, 1.0, 3.0 and 10.0 per cent with other elements at fixed values. The fact that the derived abundances of elements other than C and He may differ slightly from their assumed values is not likely to be a serious source of error. The line-formation calculations were carried out with the Uppsala LTE line-formation code EQWIDTH.

3.2 Models for $T_{eff} \ge 10000$ K

To analyse cool EHes in the temperature range $10\,000 \le T_{eff} \le 14\,000$ K, a grid of appropriate models was calculated using the model atmosphere code STERNE (Jeffery & Heber 1992). The grid provides models for temperatures in the range $10\,000 \le T_{eff} \le 40\,000$ K, and gravities in the range $1.0 \le \log g \le 8.0$ [cgs]. The relative abundances by number used for the standard grid are He = 99 per cent, H/He = 10^{-4} and C/He = 1 per cent, and the rest of the elements are solar. Models were computed in the temperature range $10\,000 \le T_{eff} \le 14\,000$ K for the following values of C/He ratios: C/He = 0.1, 0.3, 0.5, 1.0, 3.0, and 10.0 per cent, with other elements at fixed values. The opacity calculations were made after taking into account the effects of line-blanketing using the tables of opacity distribution functions for helium- and carbon-rich material. The Belfast LTE code SPECTRUM was used for line-formation calculations (Jeffery & Heber 1992; Jeffery, unpublished).

3.3 Consistency between model grids

The two model atmosphere grids do not overlap in effective temperature. To compare the grids, we derived a model for 9500 K by extrapolating the high-temperature grid models whose coolest models are at 10 000 K. The extrapolated model and an Uppsala model for 9500 K gave identical abundances to within 0.05 dex. The abundances derived for weak lines using SPECTRUM and EQWIDTH are in agreement within 0.1 dex for most of the species. We find that the abundances derived using the former are always lower than those derived using the latter. This small difference is probably due to the data used for continuous opacity being from two different sources.

3.4 Abundance analysis – some fundamentals

Attention has to be paid to both the line and the continuous opacities in extracting the abundance of an element E from lines produced by an atom, ion, or molecule of E. In the case of normal stars, hydrogen directly or indirectly exerts a major influence on the continuous opacity, with the result that analysis of lines of element E provides the abundance E/H without recourse to a direct measurement of the hydrogen abundance from H I lines. The result is dependent on the assumed He/H ratio, which is small ($\simeq 0.1$) for normal stars and unlikely to vary greatly from one normal star to the next. Since E is a minor species and He/H is effectively common to all normal stars, $A_E = E/H$ is a fair measure of abundance. Some authors prefer to quote abundance as a mass fraction, say $Z(E)$ where

$$Z(E) = \frac{\mu_E N_E}{\mu_H N_H + \mu_{He} N_{He} \ldots + \mu_i N_i}$$

$$\simeq \frac{\mu_E A_E}{1 + 4A_{He}}, \tag{1}$$

where $Z(E)$ is directly calculable from A_E, the fruits of the abundance analysis, and an assumption about A_{He}. Of course, this latter assumption may be replaced by a spectroscopic measurement in the case of hot stars whose spectra provide helium lines.

Elemental mass fraction is an invaluable quantity when the H/He ratio has been changed by the addition of nuclear-processed material from H- and He-burning layers, and comparisons are to be made between normal and peculiar stars. The number of nucleons is conserved. Changes to the hydrogen and helium abundance are unlikely to be accompanied by a change of (say) the iron content of the atmosphere, and hence the mass fraction of iron will be unaltered even though hydrogen may have been greatly depleted. In the case of cool He-rich stars like the R CrB stars, carbon is the source of the continuous opacity so that analysis of lines of E gives the ratio E/C. The mass fraction $Z(E)$ for the H-poor case is given by

$$Z(E) = \frac{\mu_E A'_E}{A'_H + 4\text{He/C} + 12\ldots + \mu_i A'_i}, \tag{2}$$

where $A'_E = E/C$. In recognition of the conservation of nucleons, it is helpful to normalize the customary abundances based on the convention that $\log \epsilon(E) = \log(E/H) + 12.0$ to a scale in which $\log \Sigma \mu_i \epsilon(i) = 12.15$, where the constant of 12.15 is derived from the solar abundances with He/H $\simeq 0.1$; we write these normalized abundances as $\log \epsilon(E)$. On this scale, if all hydrogen is converted to helium, the helium abundance is about 11.54. For approximately solar abundances, elements carbon and heavier contribute 0.01 dex or less to the sum.

Since the He/C ratio is most probably large, say about 100, $Z(E) \simeq \mu_E A'_E/(4\text{He/C})$ which is not calculable from the E/C ratio
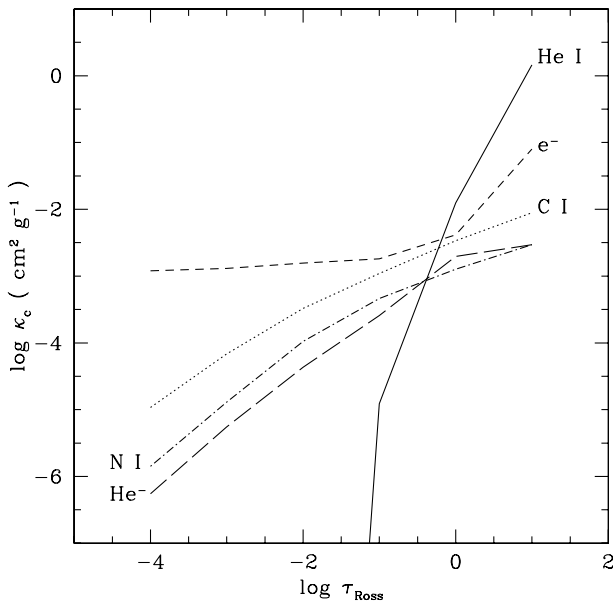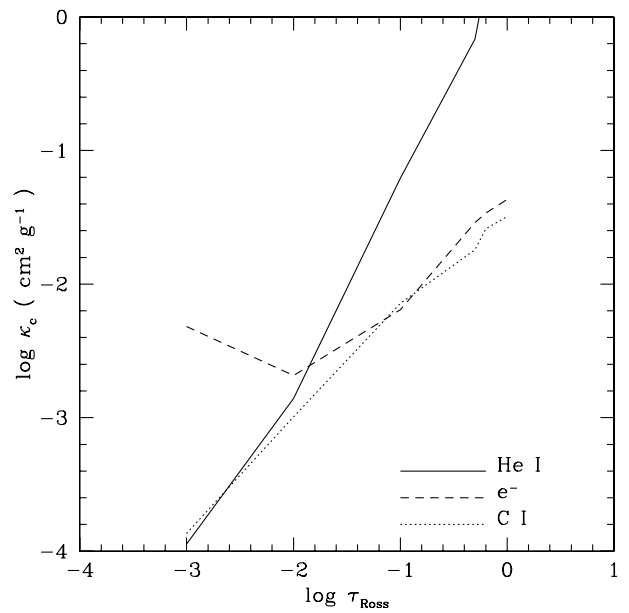
Figure 2. Dominant sources of continuous opacity at $5000\,\text{\AA}$ (κ_c) as a function of Rosseland mean optical depth (τ_{Ross}) for the model atmosphere: $T_{\text{eff}} = 9500\,\text{K}$, $\log g = 1.0$ and C/He = 1 per cent.
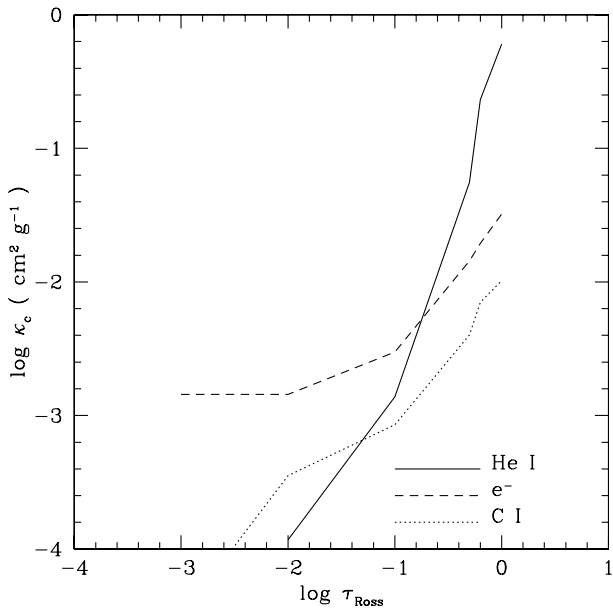
Figure 3. Dominant sources of continuous opacity at $5000\,\text{\AA}$ (κ_c) as a function of Rosseland mean optical depth (τ_{Ross}) for the model atmosphere: $T_{\text{eff}} = 11\,000\,\text{K}$, $\log g = 1.0$ and C/He = 1 per cent.

without either an assumption about or a measurement of the He/C ratio. The ratio is not spectroscopically determinable for cool H-poor stars, and there are not, unlike the He/H ratio of normal stars, astrophysical grounds for asserting that the C/He ratio is likely to have a particular value. Stellar kinematics can provide a guide for initial metallicity, and in turn constrain the He/C ratio (Rao & Lambert 1996). Of course, abundance ratios of elements E_1 and E_2 are not dependent on the unknown C/He except in so far as the model atmosphere structure is dependent on C/He.

To illustrate when the C/He ratio is or is not directly determinable from the spectrum of a H-poor star, we present the results of two calculations: an investigation of the sources of

Figure 4. Dominant sources of continuous opacity at $5000\,\text{\AA}$ (κ_c) as a function of Rosseland mean optical depth (τ_{Ross}) for the model atmosphere: $T_{\text{eff}} = 13\,000\,\text{K}$, $\log g = 2.0$ and C/He = 1 per cent.

continuous opacity, and predictions of the equivalent widths of representative lines of C I, C II and He I for model atmospheres spanning the effective temperature range of interest.

Figs 2, 3 and 4 show the run of continuous opacity at $5000\,\text{\AA}$ for the major contributors as a function of optical depth for the following model atmospheres:

(i) $T_{\text{eff}} = 9500\,\text{K}$, $\log g = 1.0$ and C/He = 1 per cent;
(ii) $T_{\text{eff}} = 11\,000\,\text{K}$, $\log g = 1.0$ and C/He = 1 per cent, and
(iii) $T_{\text{eff}} = 13\,000\,\text{K}$, $\log g = 2.0$ and C/He = 1 per cent.

Fig. 2 shows that electron scattering and photoionization of neutral carbon are the major sources of continuous opacity in the line-forming regions for model of $T_{\text{eff}} = 9500\,\text{K}$. Most of the carbon is singly ionized and contributes about half of the total free electrons. The remaining half of the free electrons come from nitrogen and oxygen. At $\log \tau = -0.25$, photoionization of carbon and helium contribute to the continuous opacity equally. Helium dominates the continuous opacity for $\log \tau$ greater than -0.25. Figs 3 and 4 show that electron scattering and photoionization of neutral helium are the major sources of continuous opacity in the line-forming regions at $T_{\text{eff}} = 11\,000$ and $13\,000\,\text{K}$. Photoionization of neutral helium contributes almost all of the free electrons. For hotter stars, e.g., BD $-1°3438$ and LS IV $-1°002$, it is evident from Figs 3 and 4 that helium controls the continuum opacity.

Predicted equivalent widths for representative lines of carbon and helium are illustrated in Fig. 5. This shows several points that were anticipated from Figs 2, 3 and 4. For cool stars, say $T_{\text{eff}} \lesssim 8000\,\text{K}$, the C I equivalent widths are almost independent of the assumed C/He ratio. The equivalent widths are also almost independent of effective temperature and surface gravity as a result of the very similar excitation potentials for the lower levels of the lines and the photoionization edges. It follows that the predicted equivalent widths of weak C I lines are essentially independent of the atmospheric parameters including the C/He ratio (Schönberner 1975). This prediction is verified by the observation that a C I line has a similar equivalent width in all R CrB stars and the coolest of our EHes (see fig. 1 in Rao & Lambert 1996). Strong C I lines are
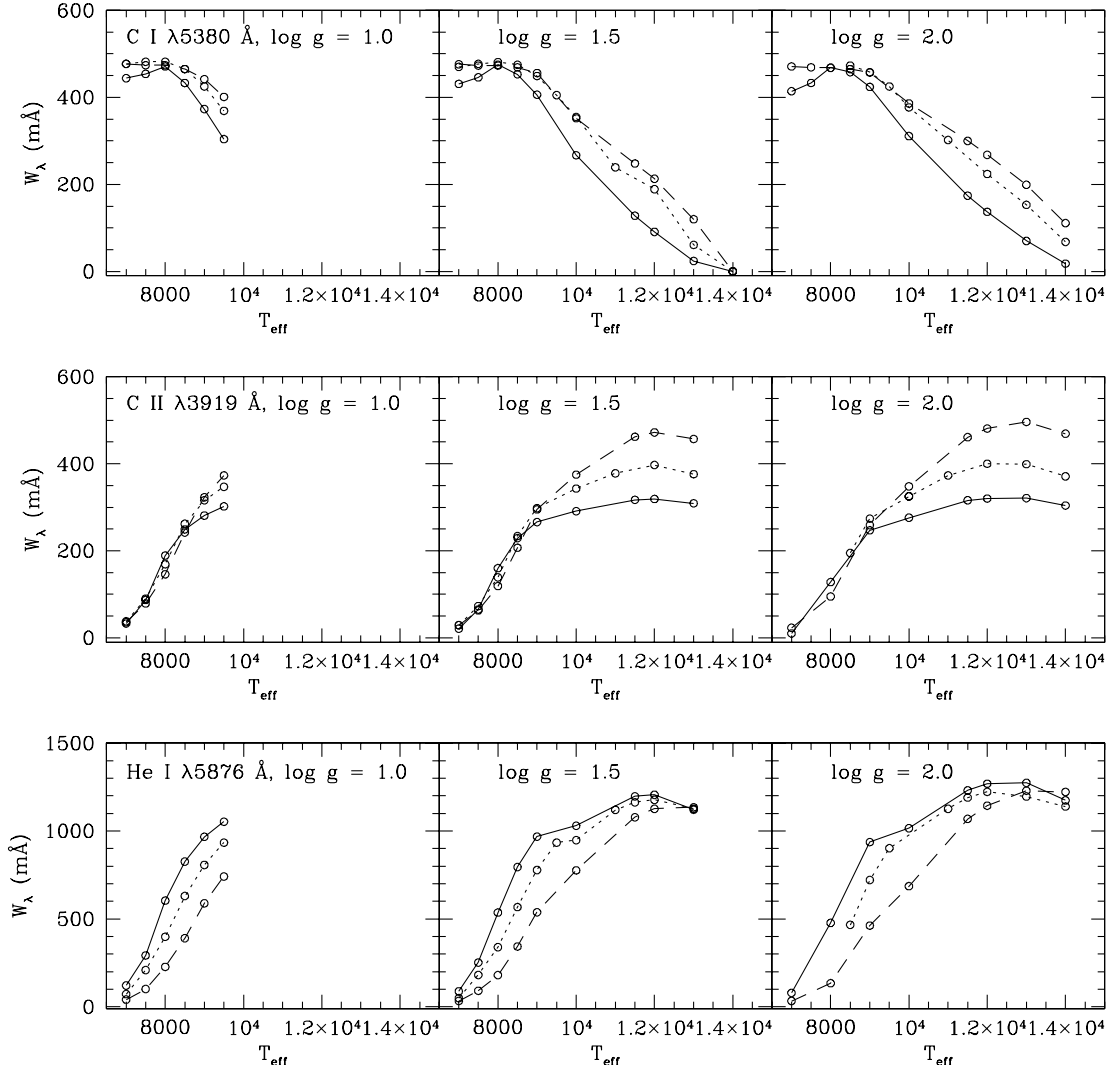
Figure 5. Predicted equivalent widths of C I, C II and He I lines plotted against T_{eff} for $\log g$ values of 1.0, 1.5 and 2.0. The solid, dotted and dashed lines represent models with C/He of 0.3, 1.0 and 3.0 per cent, respectively.

dependent on the assumed microturbulence, and, of course, an equivalent width depends on atomic data, specifically the line's *gf*-value. The C II equivalent widths are also almost independent of effective temperature, surface gravity, and the assumed C/He ratio for cool stars (see Fig. 5). A detailed comparison of predicted and observed C I equivalent widths of the R CrB stars reveals a systematic discrepancy: the observed lines are appreciably weaker than predicted. Asplund et al. (2000) dub this issue 'the carbon problem' and review several possible explanations for it. The He I lines are dependent on the C/He ratio and very sensitive to the assumed effective temperature, as the Fig. 5 shows. In the case of stars like R CrB ($T_{eff} \simeq 6800$ K), the He I lines are too weak (and blended) to be used to determine the C/He ratio.

At the hot limit of our calculations, a different situation pertains. It is the He I lines that are independent of the C/He ratio; photoionization of helium is the dominant contributor to the continuous opacity. The C I lines are weak, and sensitive to effective temperature and surface gravity; carbon is predominantly singly ionized. The C II lines are sensitive to the C/He ratio and effective temperature, but rather insensitive to the surface gravity. The temperature sensitivity of C II and He I lines is minimized around 12 000 K. At high temperatures, say $T_{eff} \gtrsim 12\,000$ K, the

He I equivalent widths are independent of the assumed C/He ratio, and insensitive to the other atmospheric parameters including the microturbulence; helium atoms have a large thermal velocity. A check on the models is then possible by comparing predicted and observed equivalent widths of the He I lines. At higher temperatures, helium becomes ionized and the equivalent width of a He I line declines as the He II lines increase in strength.

4 ABUNDANCE ANALYSIS

The analysis involves the determination of T_{eff}, surface gravity ($\log g$), and microturbulence (ξ) before estimating the photospheric elemental abundances of the star.

The microturbulence is derived by requiring that lines of all strengths for a particular species give the same value of abundance. The derived ξ is found to be independent of T_{eff}, $\log g$ and C/He, adopted for the model atmosphere (Pandey 1999).

For FQ Aqr, LS IV $-14°\,109$ and BD $-1°\,3438$ we used Fe II, Ti II, Cr II and C I lines, and for LS IV $-1°\,002$ we used Fe II, S II, N II and C I lines for determining the microturbulent velocity ξ. In the case of LS IV $-14°\,109$, Fe II, Ti II and Cr II lines gave $\xi = 6$ km s^{-1}, and C I lines a value of $\xi = 7$ km s^{-1}. We adopt the
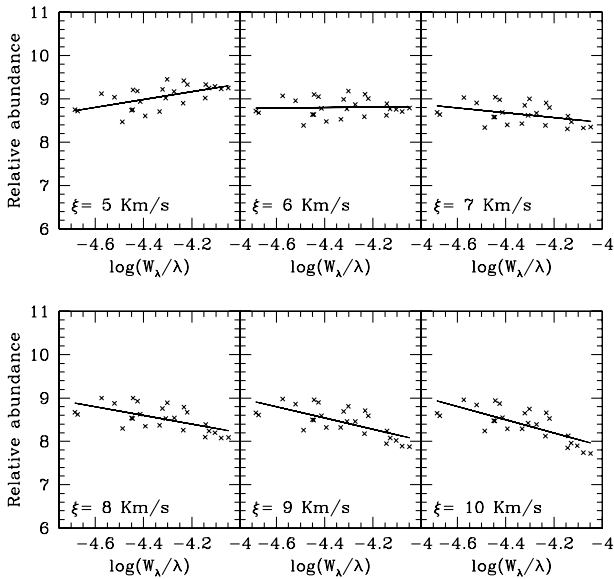
Figure 6. Relative abundances from Ti II lines for LS IV −14° 109, plotted against their line strength, represented by ($\log W_\lambda/\lambda$) for different values of ξ.

Figure 7. Excitation balance for FQ Aqr using Fe II lines.

Figure 8. Final $T_{\rm eff}$ and $\log g$ of LS IV −14° 109 with error bars.

average microturbulent velocity $\xi = 6.5 \pm 0.5\,\mathrm{km\,s^{-1}}$ (see Fig. 6). For FQ Aqr, BD −1° 3438 and LS IV −1° 002 we estimate the microturbulent velocity ξ as 7.5 ± 0.5, 10.0 ± 1.0 and $10.0 \pm 1.0\,\mathrm{km\,s^{-1}}$, respectively. The microturbulence values provided by the different elements agree well within the errors quoted above.

$T_{\rm eff}$ is estimated by requiring that the lines of a particular species but of differing excitation potentials should return the same elemental abundance. The model grid is searched for the model that satisfies this condition. The optimum $T_{\rm eff}$ is found to be independent of the adopted $\log g$ and C/He for the model atmosphere (Pandey 1999).

In all cases, Fe II lines, which are numerous and span a range of excitation potentials, were used to determine $T_{\rm eff}$. Fig. 7 illustrates the procedure used to determine $T_{\rm eff}$. No other species shows such a large range in excitation potential to determine $T_{\rm eff}$.

The surface gravity is estimated by the requirement that the model atmosphere gives the same abundances for neutral, singly ionized, and doubly ionized lines of a given element. The ionization equilibria are independent of the adopted C/He of the model atmosphere.

Since the ionization equilibrium depends on both surface gravity and temperature, its imposition defines a locus in the $\log g$–$T_{\rm eff}$ plane for a given pair of ions (or atom and ion) of an element. The ionization equilibrium of the following species (when sufficient lines are available) are used to estimate $T_{\rm eff}$ and $\log g$: S II/S I, Si III/Si II/Si I, N II/N I, Al III/Al II/Al I, C II/C I, Fe III/Fe II/Fe I, Mg II/Mg I and O II/O I. The solutions for $T_{\rm eff}$ and $\log g$ obtained for LS IV −14° 109 are shown in Fig. 8, where the ionization equilibria are shown by different line-types, and the excitation balance by arrow heads in the $T_{\rm eff}$–$\log g$ plane.

If there is an evolutionary link between our cool EHes and the hot EHes and R CrB stars, the mass M and luminosity L of the stars in the three groups should be related. One might suppose that for a particular isochrone, the mass is constant. In essence, one assumes a close relation between M and L; it is readily shown that the ratio $M/L \propto g/T_{\rm eff}^4$. Hence, as an additional locus, we show lines of constant $\log(L/M)$ in Fig. 8; the chosen values of 3.75 and 4.5 span the values of a majority of the hot EHes (Jeffery 1996), but a few
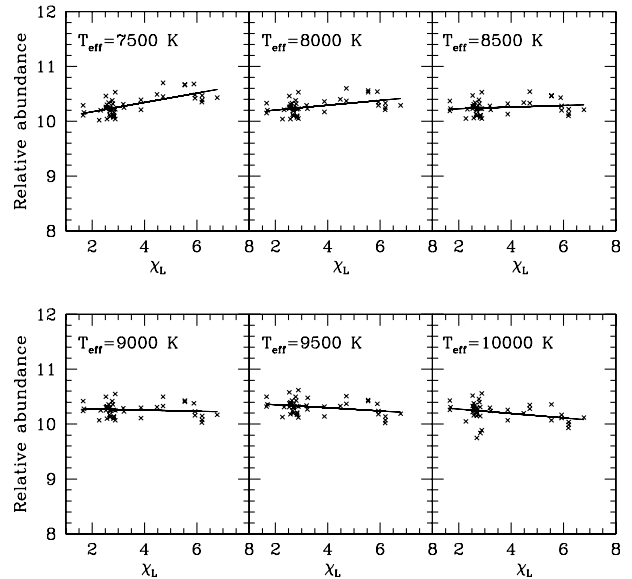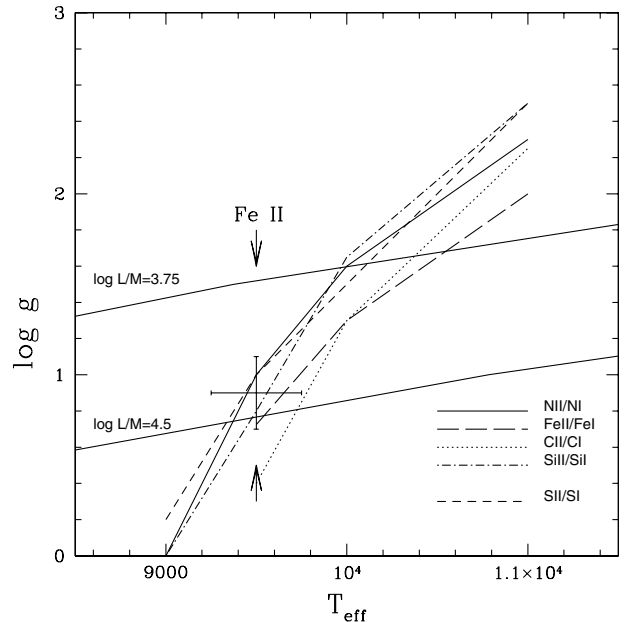
stars have a lower $\log(L/M)$. Note that we have not used these lines of constant $\log(L/M)$ in determining the $T_{\rm eff}$ and $\log g$.

Since available loci from ionization equilibrium run approximately parallel to each other, separate solutions for $T_{\rm eff}$ and $\log g$ cannot be obtained. Excitation equilibrium provides a line in the $T_{\rm eff}$ versus $\log g$ plane that intersects the ionization equilibria at a steep angle, enabling $\log g$ to be estimated. The adopted $T_{\rm eff}$ and $\log g$ are indicated on Fig. 8.

The gf-values and excitation potentials for the lines used in our LTE analysis were taken from the compilations by R. E. Luck (private communication), Jeffery (1994), Thévenin (1989, 1990) and Kurucz & Peytremann (1975). We have used the gf-values of C I lines from the Opacity project (Luo & Pradhan 1989; Hibbert et al. 1993; Seaton et al. 1994). The Stark broadening and radiation broadening coefficients were mostly taken from the compilation by

Jeffery (1994). The data for computing He I profiles are obtained from various sources. The *gf*-values are taken from Jeffery (1994), radiation broadening coefficients from Wiese, Smith & Glennon (1966), and electron broadening coefficients from the combination of Griem et al. (1962), Bassalo, Cattani & Walder (1980), Kelleher (1981) and Dimitrijevic & Sahal-Bréchot (1984). The effects of ion broadening are also included.

All the synthesized spectra corrected for the instrumental profile were convolved with a Gaussian profile to give a good fit to typical unblended line profiles. Only weak and unblended lines of trace elements were used to fix the full width at half maximum (FWHM) of the Gaussian profile. We find that the resultant FWHM of the Gaussian profile of the stellar lines used is more than the FWHM of the instrumental profile. We attribute this extra broadening to a combination of rotation and macroturbulence (see v_M in Table 1).

The stars FQ Aqr and LS IV −14° 109 were earlier analysed by Asplund et al. (2000) based on spectra with a resolution of 30 000 obtained at CTIO in the wavelength region 5500 to 6800 Å. The present analysis is based on new higher resolution spectra covering 3800 to 10 000 Å, providing more spectral lines of many more species.

4.1 FQ Aqr

The Fe II lines require that $T_{eff} = 8750 \pm 250$ K. Lines stronger than 200 mÅ were rejected. Ionization equilibria involving N, Al, Mg, S and Fe were considered. The S II/S I ionization balance is given highest weight, because the lines of S II and S I identified in the spectra are weak. The C II/C I ionization balance is given a lower weight because of the potential carbon problem (see below). A lower weight is also given to the Al II/Al I ionization balance, because we have only one line of Al I and the *gf*-values for Al II lines may be unreliable. Equal weights are given to the ionization balance of N II/N I, Mg II/Mg I and Fe II/Fe I. The spread in these loci is similar to that found for the hot EHes – see, e.g., Jeffery (1998). We adopt $T_{eff} = 8750 \pm 250$ K and $\log g = 0.75 \pm 0.25$ (Table 1).
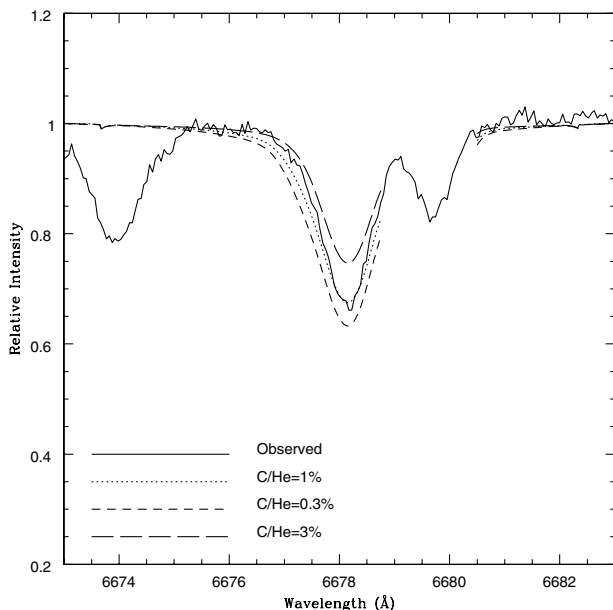
Figure 9. Observed and synthesized He I λ6678 Å line profile of FQ Aqr. The He I line profiles are synthesized using models of $T_{eff} = 8750$ K and $\log g = 0.75$, but for different values of C/He.

At the T_{eff} of FQ Aqr, carbon is predicted to be the leading contributor to the continuous opacity (Fig. 2). Under these circumstances, the He I lines are sensitive to the C/He ratio (Fig. 5) which may be derived by fitting the He I lines at 5048, 5876 and 6678 Å (Fig. 9). The lines give C/He = 1.2 ± 0.2 per cent, where the uncertainty reflects only the scatter of the three results. Temperature and gravity errors contribute about ±0.7 per cent to the C/He ratio. The error in microturbulence contributes a negligible amount of uncertainty to the C/He ratio.

For the adopted model, the predicted equivalent widths of C I and C II lines are almost independent of the model's assumed C/He ratio as long as C/He exceeds the minimum necessary for carbon to dominate the continuous opacity (C/He ≳ 0.5 per cent). Then there are essentially no free parameters with which to adjust the predicted equivalent width of a carbon line with a given *gf*-value. Comparison of predicted and observed equivalent widths of FQ Aqr shows, as it did for the R CrB stars (Asplund et al. 2000), that observed equivalent widths of the C I lines are weaker than predicted. For example, models with the adopted T_{eff} and $\log g$ require the C abundance (or *gf*-value) to be reduced by about 0.4 dex for both C/He = 3 and 1 per cent models. However, for the C/He = 0.3 per cent model, the difference is a mere 0.06 dex. At this C/He ratio, carbon is not the dominant source of continuous opacity; instead, electron scattering (most of the free electrons are coming from nitrogen and oxygen) is the major source of continuum opacity. To match the observed equivalent widths of the C II lines, models with the adopted T_{eff} and $\log g$ require the C abundance (or *gf*-value) to be reduced by about 0.2 dex for both C/He = 3 and 1 per cent models. At C/He = 0.3 per cent, predicted and observed equivalent widths agree to better than 0.05 dex. Temperature and gravity errors contribute about ±0.3 dex to the C/He ratio derived using C II lines.

If C/He ≳ 0.3 per cent, there is a carbon problem whose resolution is presumably closely related to the unidentified solution to the carbon problem of the R CrB stars. The problem is greater for C I lines than for the C II lines, a result also found for the R CrB stars. The magnitude of the problem at a given C/He ratio is smaller than for the R CrB stars, and vanishes at a higher C/He ratio than for the R CrB stars. To within the uncertainties allowed by the model atmosphere parameters, a ratio C/He ≈ 0.5 per cent produces a tolerable fit to the He I, C I and C II lines. The final abundances, as given in Table 2, are derived for C/He = 0.5 per cent.

4.2 LS IV −14° 109

The adopted atmospheric parameters (Table 1) are based on the excitation and ionization equilibria shown in Fig. 8. The $T_{eff} = 9500 \pm 250$ K is provided from the excitation of Fe II lines. The loci corresponding to ionization equilibria for five sets of atoms and ions are remarkably consistent; three are essentially identical. Equal weights are given to the ionization balance of N II/N I, Fe II/Fe I, Si II/Si I and S II/S I.

The C/He ratio is found from a fit to He I profiles. We have synthesized the 3872 and 5048 Å lines. Unfortunately, the 5876 and 6678 Å lines are not on our spectra, and the 7065 Å line is blended with telluric H_2O lines. A value C/He = 1.2 ± 0.2 per cent is obtained. Temperature and gravity errors contribute about ±0.6 per cent to the C/He ratio. The error in microturbulence contributes a negligible amount of uncertainty to the C/He ratio.

The C I lines as analysed with the C/He = 1 per cent model give an abundance corresponding to C/He = 0.75 ± 0.3 per cent. When

**Table 2.** The individual elemental abundances derived for each ion for the analysed EHe stars.

	FQ Aqr	LS IV −14° 109	BD −1° 3438	LS IV −1° 002	Sun
T_{eff} (K)	8750	9500	11750	12750	
$\log g$ (cgs units)	0.75	0.9	2.3	1.75	
C/He	0.5%	1%	0.2%	0.6%	
ξ (km s^{-1})	8.0	6.0	10.0	10.0	
H I	6.2(1)	6.2(1)	5.6(1)	7.1(1)	12.0
He I	11.54(3)	11.54(2)	11.54(2)	11.54(1)	10.99
C I	9.0 ± 0.14(30)	9.4 ± 0.16(25)	9.0 ± 0.17(28)	9.3 ± 0.15(15)	8.55
C II	9.0 ± 0.10(2)	9.5 ± 0.06(3)	8.8 ± 0.06(2)	9.3 ± 0.13(7)	
N I	7.1 ± 0.20(5)	8.6 ± 0.28(10)	8.4 ± 0.20(11)	8.2 ± 0.10(6)	7.97
N II	7.2 ± 0.07(2)	8.6 ± 0.18(5)	8.6 ± 0.15(9)	8.3 ± 0.20(14)	
O I	8.9 ± 0.15(8)	8.5 ± 0.16(8)	8.4 ± 0.19(6)	8.8 ± 0.15(3)	8.87
O II	...	...	...	8.9 ± 0.05(5)	
Ne I	7.9 ± 0.25(14)	9.4 ± 0.26(13)	8.8 ± 0.14(9)	9.0 ± 0.13(9)	8.10
Na I	5.5 ± 0.26(2)	6.8 ± 0.22(4)	6.3(1)	6.5(1)	6.33
Mg I	5.5 ± 0.12(5)	6.9 ± 0.26(2)	...	...	7.58
Mg II	6.0 ± 0.11(6)	7.3 ± 0.10(3)	6.9 ± 0.03(3)	6.9 ± 0.23(6)	
Al II	4.7 ± 0.18(4)	7.1 ± 0.2(7)	6.0 ± 0.20(8)	5.4 ± 0.17(8)	6.47
Al III	...	6.7 ± 0.10(2)	...	...	
Si I	...	7.6 ± 0.21(5)	...	...	7.55
Si II	6.3 ± 0.24(6)	7.8 ± 0.24(3)	6.5 ± 0.14(5)	5.9 ± 0.10(3)	
P II	4.2 ± 0.23(2)	5.3 ± 0.27(3)	5.3 ± 0.23(3)	5.1 ± 0.11(3)	5.50
S I	6.1 ± 0.15(3)	7.6 ± 0.24(4)	...	...	7.23
S II	5.9 ± 0.16(7)	7.5 ± 0.40(12)	6.9 ± 0.20(18)	6.7 ± 0.20(35)	
Ca I	4.0(1)	5.5(1)	...	...	6.36
Ca II	4.2(1)	5.6 ± 0.22(2)	5.5 ± 0.10(2)	5.8 ± 0.05(2)	
Sc II	2.1 ± 0.12(7)	3.3 ± 0.21(5)	...	...	3.17
Ti II	3.2 ± 0.25(42)	4.3 ± 0.21(25)	4.6 ± 0.28(18)	4.7 ± 0.14(5)	5.02
Cr I	4.0(1)	...	...	...	5.69
Cr II	3.6 ± 0.13(30)	5.1 ± 0.24(30)	4.9 ± 0.27(23)	...	
Mn II	4.3 ± 0.23(3)	5.3 ± 0.27(11)	5.1 ± 0.10(4)	...	5.47
Fe I	5.1 ± 0.12(7)	6.8 ± 0.17(7)	7.1 ± 0.04(4)	...	7.50
Fe II	5.4 ± 0.12(59)	7.0 ± 0.21(47)	6.7 ± 0.20(45)	6.3 ± 0.12(22)	
Fe III	...	...	...	6.1 ± 0.22(2)	
Ni I	...	6.6 ± 0.17(4)	...	...	6.25
Sr II	0.5 ± 0.03(2)	2.6 ± 0.05(2)	2.8 ± 0.03(2)	2.7 ± 0.20(2)	2.97
Y II	...	1.9 ± 0.17(3)	...	...	2.24
Zr II	0.8 ± 0.24(2)	1.9 ± 0.10(2)	...	...	2.60
Ba II	0.5(1)	1.7 ± 0.13(3)	...	...	2.13

uncertainties attributable to the atmospheric parameters (temperature, gravity and microturbulence) are considered, this result is consistent with that derived from the He I lines. Analysis of the C II lines with C/He = 1 per cent model gives C/He = 0.9 ± 0.25 per cent for the adopted model, where the errors reflect the uncertainty in the estimated T_{eff} and $\log g$. The abundances are derived for C/He = 1 per cent, which provides an acceptable fit to the He I, C I and C II lines.

4.3 BD −1° 3438

In deriving the atmospheric parameters (Table 1), equal weights are given to the ionization balance of N II/N I, Fe II/Fe I and C II/C I. Helium is the major contributor of continuum opacity, and hence the He I equivalent widths are almost independent of the C/He ratio. The observed profiles of the He I 5048 and 5876 Å lines are well fitted by the predictions for the T_{eff} = 11 500 K and $\log g$ = 2.0 model within errors (Fig. 10); there is no helium problem analogous to the carbon problem as seen for R CrB stars.

With He providing the continuous opacity, the C I and C II lines provide a measure of the C/He ratio. The C I lines give $\log \epsilon$(C) = 8.95 ± 0.27. Two C II lines give 8.8 ± 0.08. The C I and C II lines are in fair agreement, and imply a C/He = 0.2 ± 0.03 per cent. Temperature and gravity errors are included.
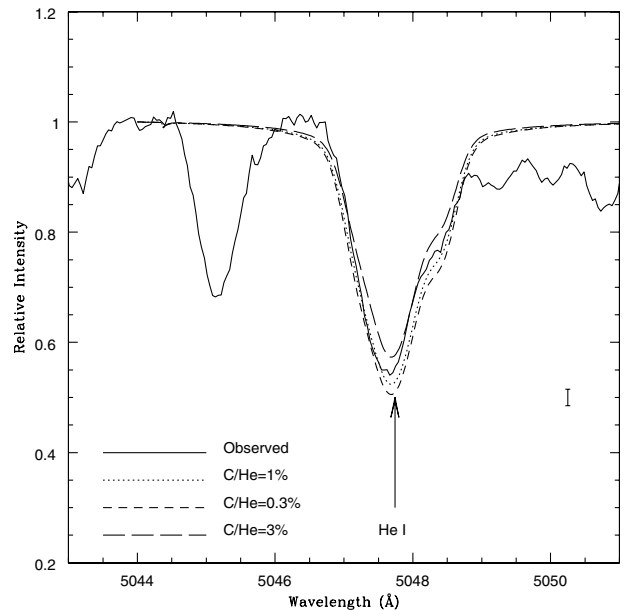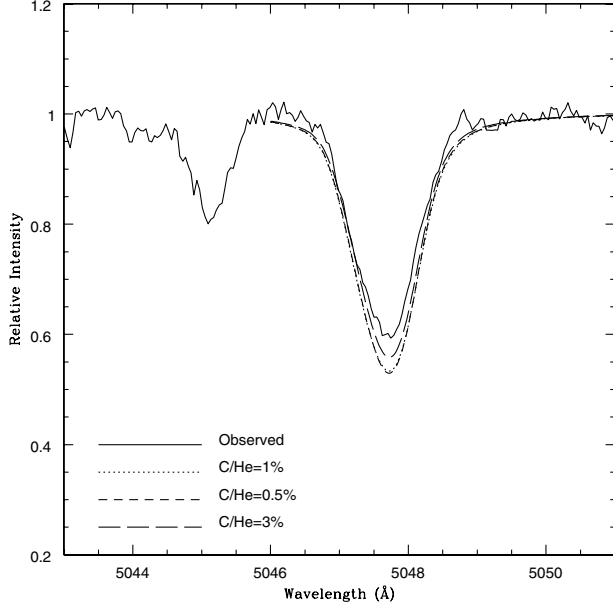

Figure 10. Observed and synthesized He I λ5047.74 Å line profile of BD −1° 3438. The He I line profiles are synthesized using the model of T_{eff} = 11 500 K and $\log g$ = 2.0, for different values of C/He. The uncertainty on the ordinate is shown by the error bar.

By definition, the carbon problem is not apparent for atmospheres for which carbon is not the dominant opacity source.

4.4 LS IV −1° 002

The adopted T_{eff} and $\log g$ using the excitation and ionization balance criteria are given in Table 1. The derived T_{eff} from the excitation balance of Fe II lines is $12\,750 \pm 250$ K. Ionization equilibria for six elements are available. Equal weights are given to the ionization balance of O II/O I, N II/N I, Fe III/Fe II and C II/C I.

Figure 11. Observed and synthesized He I λ5047.74 Å line profile of LS IV −1° 002. The He I line profiles are synthesized using the model of $T_{eff} = 13\,000$ K and $\log g = 2.0$, for different values of C/He.

Smaller weights are given to the ionization balance of Si III/Si II and Al III/Al II, because the lines available are very few and the sources of *gf*-values for these lines are not reliable.

The He I profiles are effectively independent of the C/He ratio – see Fig. 11 where we show good agreement between the predicted and observed 5048 Å profiles.

The C I lines give a C abundance equivalent to C/He = 0.6 ± 0.2 per cent. At this temperature, the spectrum of C II is well represented: seven lines give C/He = 0.6 ± 0.2 per cent. Temperature and gravity errors are included. We adopt C/He = 0.6 per cent.

5 ABUNDANCES

The final abundances were calculated using models of C/He = 0.5, 1.0, 0.2 and 0.6 per cent for FQ Aqr, LS IV −14° 109, BD −1° 3438 and LS IV −1° 002, respectively. Detailed line lists (see for SAMPLE Table A1) are available in electronic form as supplementary material on *Synergy*.

For the adopted stellar parameters, the individual elemental abundances listed in Table 2 are given as $\log \epsilon(i)$, normalized such that $\log \Sigma \mu_i \epsilon(i) = 12.15$. The abundances determined from the neutral and ionized species of an element are separately listed. The number of lines used in our analysis is given within brackets. The errors quoted are mainly due to line-to-line scatter of the abundances. The error in abundances due to the uncertainty in the adopted stellar parameters is discussed in Appendix A. Solar abundances from Grevesse, Noels & Sauval (1996) are also shown in Table 2.

Hydrogen is present in the atmospheres of these stars. We have identified four Balmer lines (Hα, Hβ, Hγ and Hδ) in our spectra. Our H abundance is based on the Hα line, but Hβ gives a consistent result. We have not used the Hγ and Hδ lines, because they are blended and noisy. Line broadening for Balmer lines was considered in determining the H abundance.

Table 3. The mean abundances $\log \epsilon(el)$ and the mean abundance ratios [*el*/Fe] for cool EHe (excluding FQ Aqr), hot EHe (excluding V652 Her and HD 144941) and majority class R CrB stars. The dispersion σ and the number of stars (#) are also given.

Element(*el*)	cool EHes			hot EHes			majority R CrB stars		
	$\log \epsilon(el)$ (σ)	[*el*/Fe] (σ)	#	$\log \epsilon(el)$ (σ)	[*el*/Fe] (σ)	#	$\log \epsilon(el)$ (σ)	[*el*/Fe] (σ)	#
H	6.3 (0.8)	−4.8 (1.2)	3	8.0 (0.5)	−3.4 (0.7)	10	6.1 (1.0)	−4.9 (1.1)	13
C	9.2 (0.4)	1.6 (0.6)	3	9.3 (0.2)	1.5 (0.3)	10	8.9 (0.2)	1.4 (0.2)	14
N	8.5 (0.2)	1.4 (0.3)	3	8.3 (0.4)	0.9 (0.3)	10	8.6 (0.2)	1.6 (0.3)	14
O	8.6 (0.3)	0.6 (0.7)	3	8.6 (0.3)	0.3 (0.6)	10	8.2 (0.5)	0.3 (0.6)	14
Ne	9.1 (0.3)	1.8 (0.5)	3	9.2 (0.3)	1.5 (0.3)	3	8.3	1.2	1
Na	6.5 (0.3)	1.1 (0.5)	3	...	...	...	6.1 (0.2)	0.8 (0.1)	13
Mg	7.0 (0.2)	0.3 (0.4)	3	7.6 (0.3)	0.6 (0.4)	10	6.7 (0.3)	0.0 (0.4)	3
Al	6.2 (0.9)	0.5 (0.5)	3	6.1 (0.5)	0.2 (0.4)	10	6.0 (0.3)	0.5 (0.3)	12
Si	7.4 (0.3)	0.8 (0.4)	3	7.4 (0.4)	0.5 (0.4)	10	7.1 (0.2)	0.6 (0.2)	14
P	5.2 (0.1)	0.6 (0.4)	3	5.7 (0.5)	0.8 (0.5)	10	5.9	1.4	1
S	7.0 (0.4)	0.7 (0.3)	3	7.1 (0.3)	0.5 (0.5)	10	6.9 (0.4)	0.7 (0.3)	14
Ca	5.6 (0.2)	0.1 (0.6)	3	6.4 (0.4)	0.5 (0.1)	7	5.4 (0.2)	−0.1 (0.2)	14
Sc	3.3	0.6	1	3.2 (1.6)	0.4 (0.9)	2	2.9 (0.3)	0.7 (0.4)	4
Ti	4.5 (0.2)	0.4 (0.7)	3	5.0 (0.8)	0.3 (0.3)	3	4.0 (0.2)	0.0 (0.3)	6
Cr	5.0 (0.1)	−0.1 (0.0)	2	5.6 (0.8)	0.4 (0.1)	2	...	...	...
Mn	5.2 (0.1)	0.3 (0.0)	2	5.3 (1.3)	0.3 (0.6)	2	...	...	...
Fe	6.6 (0.5)	0.0	3	6.9 (0.3)	0.0	10	6.5 (0.3)	0.0	14
Ni	...	...	...	5.8 (1.0)	0.1 (0.3)	2	5.8 (0.2)	0.6 (0.2)	14
Zn	...	...	...	...	...	...	4.4 (0.3)	0.7 (0.2)	11
Sr	2.7 (0.1)	0.6 (0.5)	3	...	...	...	...	...	...
Y	1.9	0.2	1	...	...	...	2.1 (0.5)	0.9 (0.4)	14
Zr	1.9	−0.2	1	...	...	...	2.1 (0.4)	0.4 (0.5)	6
Ba	1.7	0.1	1	...	...	...	1.5 (0.5)	0.4 (0.4)	14

The difference in abundances reported by Asplund et al. (2000) and our analyses of FQ Aqr and LS IV $-14°\,109$ is essentially due to differences in adopted stellar parameters.

6 COOL EHE, HOT EHE, AND R CRB STARS – COMPOSITIONS

The chemical compositions of the cool EHes are clues to the history of these enigmatic stars, which assuredly began life as normal stars with a H-rich atmosphere. Our discussion begins with a comparison of the cool EHes with their putative relatives the hot EHes and the R CrB stars. Data on the composition of hot EHes are taken from Jeffery's (1996) review and subsequent papers: Harrison & Jeffery (1997), Jeffery & Harrison (1997), Drilling et al. (1998), Jeffery (1998), Jeffery et al. (1998) and Jeffery et al. (1999). We exclude from consideration the hydrogen-deficient binaries such as υSgr, which have normal carbon abundances. Chemical compositions of the R CrB stars are taken from Asplund

et al. (2000). Our goal is to elucidate similarities, differences, and trends. It has, of course, to be kept in mind that not only evolutionary associations but also systematic errors may provide variable signatures across the collection of stars running from extreme helium stars as hot as $T_{eff} = 30\,000$ K to cool R CrB stars with $T_{eff} = 6000$ K, and with surface gravities from $\log g \simeq 1$ to 4.

Mean abundances for the three groups are given in Table 3, where the dispersion σ is a measure of the range of the published abundances. For the R CrB stars, the given carbon abundance is the spectroscopic carbon abundance, which is 0.6 dex lower than the input carbon abundance used for the model. We give both $\log\epsilon(el)$ and [el/Fe]. From this table, we exclude FQ Aqr, four minority class R CrB stars, and the hot R CrB star DY Cen (Jeffery & Heber 1993), because these stars show a much lower Fe abundance and, in some cases, other striking abundance anomalies. The minority class R CrB stars show lower Fe abundance and higher Si/Fe and S/Fe ratios than majority class R CrB stars (Asplund et al. 2000). Abundances for these stars are summarized in Table 4. Models of

Table 4. The abundances $\log\epsilon(el)$ and the abundance ratios [el/Fe] for minority class R CrB stars (V CrA, VZ Sgr, V3795 Sgr and V854 Cen), the hot R CrB star DY Cen, and the cool EHe star FQ Aqr.

el	V CrA		VZ Sgr		V3795 Sgr		V854 Cen		DY Cen		FQ Aqr	
	abun[a]	[el/Fe]	abun[a]	[el/Fe]	abun[a]	[el/Fe]	abun[a]	[el/Fe]	abun[a]	[el/Fe]	abun[a]	[el/Fe]
H	8.0	−2.0	6.2	−4.1	<4.1	−6.0	9.9	−0.6	10.8	1.3	6.2	−3.7
C	8.6	2.1	8.8	2.0	8.8	2.2	9.6	2.6	9.5	3.5	9.0	3.0
N	8.6	2.6	7.6	1.3	8.0	1.9	7.8	1.3	8.0	2.5	7.2	1.2
O	8.7	1.8	8.7	1.5	7.5	0.5	8.9	1.5	8.6	2.2	8.9	2.2
Ne	…	…	…	…	7.9	1.7	…	…	9.6	4.0	7.9	1.9
Na	5.9	1.6	5.8	1.2	5.9	1.5	6.4	1.6	…	…	5.5	1.3
Mg	6.6	1.0	…	…	6.1	0.4	6.2	0.1	7.3	2.2	6.0	0.6
Al	5.3	0.8	5.4	0.6	5.6	1.0	5.7	0.7	5.9	1.9	4.7	0.2
Si	7.6	2.0	7.3	1.4	7.5	1.8	7.0	0.9	8.1	3.1	6.3	0.9
P	…	…	…	…	6.5	2.9	…	…	5.8	2.8	4.2	0.8
S	7.5	2.3	6.7	1.2	7.4	2.1	6.4	0.7	7.1	2.4	6.0	0.9
Ca	5.1	0.7	5.0	0.3	5.3	0.8	5.1	0.2	…	…	4.2	−0.1
Sc	2.8	1.6	…	…	2.8	1.5	2.9	1.2	…	…	2.1	1.1
Ti	3.3	0.3	…	…	3.5	0.4	4.1	0.6	…	…	3.2	0.3
Cr	…	…	…	…	…	…	4.2	…	…	…	3.7	0.1
Mn	…	…	…	…	…	…	…	…	…	…	4.3	0.9
Fe	5.5	0.0	5.8	0.0	5.6	0.0	6.0	0.0	5.0	0.0	5.4	0.0
Ni	5.6	1.4	5.2	0.6	5.8	1.5	5.9	1.2	…	…	…	…
Zn	2.9	0.3	3.9	1.0	4.1	1.4	4.4	1.3	…	…	…	…
Sr	…	…	…	…	…	…	2.2	0.7	…	…	0.5	−0.3
Y	0.6	0.4	2.8	2.3	1.3	1.0	2.2	1.5	…	…	…	…
Zr	…	…	2.6	1.7	…	…	2.1	1.0	…	…	0.8	0.3
Ba	0.7	0.6	1.4	1.0	0.9	0.7	1.3	0.7	…	…	0.5	0.4

[a] abun = $\log\epsilon(el)$

Table 5. The mean abundance ratios el/S for cool EHes (including FQ Aqr), hot EHes (excluding V652 Her and HD 144941) and majority class R CrB stars. The dispersion σ is given in parentheses.

Ratio	hot Ehe	cool EHe	majority R CrB	Normal Star	
				Sun	[Fe/H] = −1
Na/S	…	−0.6 (0.2)	−0.8 (0.3)	−0.9	−0.6
Mg/S	0.5 (0.2)	−0.1 (0.3)	…	0.4	0.4
Al/S	−1.1 (0.3)	−0.9 (0.3)	−1.0 (0.3)	−0.8	−0.5
Si/S	0.3 (0.3)	−0.2 (0.5)	0.3 (0.2)	0.3	0.3
P/S	−1.4 (0.4)	−1.8 (0.3)	…	−1.7	−1.5:
Ar/S	−0.7 (0.1)	…	…	−0.7	−0.7
Ca/S	−0.9 (0.1)	…	−1.5 (0.3)	−0.9	−0.9
Ti/S	−2.5 (0.5)	−2.6 (0.5)	−2.9 (0.2)	−2.2	−2.2
Fe/S	−0.1 (0.3)	−0.5 (0.4)	−0.4 (0.3)	0.3	−0.1
Ni/S	…	…	−1.0 (0.3)	−1.0	−1.4
Zn/S	…	…	−2.6 (0.3)	−2.6	−3.0

C/He = 1 per cent are used to derive the abundances of R CrB stars except for V854 Cen for which a C/He = 10 per cent model is used (see Asplund et al. 1998).

The mean abundances of α-elements relative to Fe for the three groups are not as expected for their mean Fe abundances (Table 3). Relative to sulphur, mean abundances for the three groups are given in Table 5 for elements from sodium through to the iron group which were measured in 40 per cent or more of the stars comprising each group. Sulphur is chosen as the reference element in preference to iron, the customary choice, for reasons outlined below. The dispersion σ given in parentheses for each entry is probably dominated by the measurement errors. Table 5 also gives the solar ratios and those expected of a normal star with [Fe/H] = −1 (Lambert 1989; Goswami & Prantzos 2000; Wheeler, Sneden & Truran 1989). We have assumed that the abundances of the α-elements Mg, Si, S, Ca and Ti vary in concert with decreasing [Fe/H]. There are no observations of P in stars, but we assume [P/Fe] increases less steeply than [S/Fe] with decreasing [Fe/H]. FQ Aqr is included under cool EHes in Table 5.

6.1 The C/He ratios

With two exceptions, the C/He ratios of the hot EHes are in the range 0.3 to 1.0 per cent for a mean of 0.7 per cent. Our cool EHes including FQ Aqr have C/He ratios in the same range, as does the hot R CrB star DY Cen. The hot EHes with a C/He ratio quite different from the mean are V652 Her and HD 144941 with C/He $\simeq$ 0.003 per cent. This pair also show other differences with respect to the hot EHes. The hot R CrB star MV Sgr has a low ratio of C/He $\simeq$ 0.02 per cent. The C/He ratio is not directly determinable for the cool R CrB stars.

It is a remarkable result that, except for three stars with a very low C/He ratio, the C/He ratio is uniform to within a factor of 3 despite large variations in other elemental abundances affected by nuclear burning of H and He.
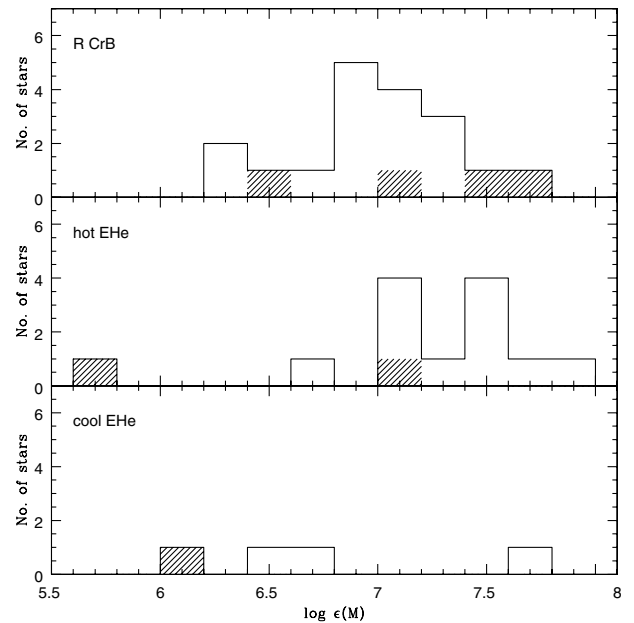
6.2 Metallicity

Products of hydrogen- and helium-burning are clearly present in the atmospheres of the H-poor stars. To assess the initial metallicity of the stars, it is necessary to consider elements unaffected by these burning processes. Synthesis of elements from silicon through to the iron group occurs in advanced burning stages and is followed by an explosion. Hence we assume that their abundance expressed as a mass fraction is preserved and so indicates a star's initial metallicity. There are three caveats: (i) synthesis of these elements may occur in a companion star that explodes and dumps debris on to the star that is or becomes the H-poor star, (ii) severe exposure to neutrons will convert iron-peak and lighter nuclei to heavier elements such as Y and Ba, and (iii) the abundances may be distorted by non-nuclear processes. Israelian et al. (1999) propose the first of these scenarios to account for the composition of the main-sequence companion to a low-mass X-ray binary, but in this case the affected star is not demonstrably H-poor. Conversion of Fe to heavy elements would create enormous overabundances of the heavy elements. Giridhar, Lambert & Gonzalez (2000) discuss how dust–gas separation has affected the atmospheric composition of certain RV Tauri variables. Gravitational settling and radiative diffusion are other processes that can distort chemical compositions.

Of the potential indicators of a star's initial metallicity, Si, S, Ca, Ti and Fe have been measured across the EHes and R CrB stars (see
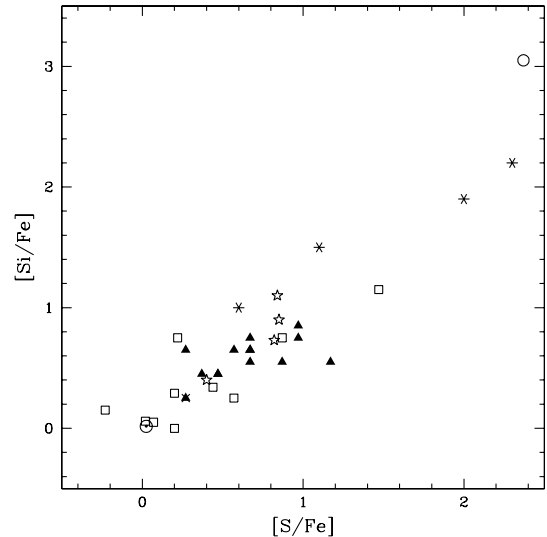
Figure 12. [Si/Fe] versus [S/Fe] for cool EHe, majority and minority class R CrB stars and hot EHes: Symbols: ☆ represent cool EHes, □ hot EHes, ▲ majority class R CrB stars, * minority class R CrB stars, ○ DY Cen, and × V652 Her with low C/He (~0.003 per cent). The Sun is denoted by ⊙.

Figure 13. A frequency histogram of the initial metallicity M for R CrB, hot EHes and cool EHes. The hatched stars represent the minority class R CrB stars, the cool EHe star FQ Aqr, the hot R CrB star DY Cen, and the hot EHe star HD 144941 with low C/He content (~0.003 per cent).

Table 3). Table 5 shows that abundance ratios with respect to S are normal across the groups, with the following exceptions: Ca/S, Ti/S, and Fe/S are 0.3 to 0.7 dex lower for the majority R CrB stars than expected for normal stars of any metallicity. To within the dispersions, the same ratios for the EHes are at their expected values. The R CrB stars also show a higher Ni/Fe ratio than expected. In the light of the Ca, Ti, Fe and Ni abundances for the R CrB stars, we elect to identify Si and S as providing the initial metallicity ([M/H], where M ≡ Fe), which we find from relations between [Si/Fe] or [S/Fe] and [Fe/H] for normal stars. The mean

[Fe/H] obtained from these two relations for a given Si and S abundance is represented as [M/H]. Note that the Si/S ratio is normal across the entire sample; the apparently low Si/S ratio of cool EHes has a large dispersion. Relative to M, the majority R CrB stars are Ca-, Ti-, and Fe-deficient but Ni-rich. These 'anomalies' may reflect either systematic errors in the abundance analyses of (presumably) the R CrB stars, and/or real differences between the EHes and the R CrB stars. The fact that the Si/Fe and S/Fe ratios are increased greatly for the minority R CrB stars and FQ Aqr (Table 4) suggests that systematic errors are not the sole explanation for the higher ratios of the majority R CrB stars; physical parameters of Table 4's denizens overlap those of the majority R CrB stars and the EHes. Fig. 12 shows the [Si/Fe] versus [S/Fe]. It is difficult to suppress the hunch that the Fe abundance has been altered for stars in Table 4, and possibly for some stars contributing to Table 3. Other elements, including Si and S, may have been affected to a lesser degree. Adopting M as the initial metallicity, we show in Fig. 13 histograms for EHes and R CrB stars; the mean values of M are slightly subsolar.

To confirm the slight metal deficiency, we consider the Galactic distribution of the stars. We have estimated the mean vertical height $|z|$ and space motions (U, V, W) for 15 R CrB stars. Distances were estimated assuming $M_V = -4.5 \pm 0.5$, and $E(B - V)$ values were taken from Asplund et al. (1997a). Proper motions and radial velocities were obtained from SIMBAD, and Asplund et al. (2000), respectively. For the R CrB stars, we find $|z| \simeq 550$ pc with the high-velocity, high-z star UX Ant excluded. The mean Galactic rotation velocity $\langle V_{\rm rot} \rangle$ is about 180^{+20}_{-60} km s^{-1} which, according to Chiba & Yoshii (1998), implies [Fe/H] $\simeq -0.6^{+0.3}_{-0.2}$ or $\log \epsilon$(M) $\simeq 6.9^{+0.3}_{-0.2}$, a value roughly consistent with M from Fig. 13 within errors. Two exceptions, UX Ant and VZ Sgr, are high-velocity stars, and not surprisingly are quite metal-poor.

Distances and the $|z|$ for most EHes were taken from Heber & Schönberner (1981). For stars not in their list, we assumed $\log L/L_\odot = 4.1$ to calculate distances. Radial velocities were taken from Jeffery, Drilling & Heber (1987). We did not consider LSS 3184, LS IV +6°002, HD 144941 and V652 Her, because they have lower L/M values. The Galactic rotation velocity of 160^{+40}_{-100} km s^{-1} implies $\log \epsilon$(M) $\simeq 6.7^{+0.5}_{-0.3}$, a value roughly consistent with M from Fig. 13.

In the discussion of the abundances, we adopt M ($\equiv$ Fe) derived from the Si and S abundances, using [Si/Fe] and [S/Fe] versus [Fe/H] relations for normal stars, as the primary measure of a star's initial metallicity, but note in several places how adoption of the Fe abundances affects our conclusions.

6.3 Hydrogen

Of the chemical elements, hydrogen shows the greatest abundance variation across the EHe – R CrB sample: the most H-rich star is the hot R CrB star DY Cen with $\log \epsilon$(H) $= 10.7$ and the least H-rich stars are the R CrB stars XX Cam and the minority member V3795 Sgr with $\log \epsilon$(H) ≤ 4. For the majority R CrB stars, the spread is from 7.4 for SU Tau to the upper limit of 4.1 for XX Cam. The hot EHes have a higher maximum H abundance: five of the six stars with detectable Balmer lines have an abundance higher than that of the majority R CrB stars. The lower bounds on the H abundance may not differ: the upper limit to the H abundance is comparable to the abundance in SU Tau for four hot EHes. The two hot EHes (V652 Her and HD 144941) with a very low C/He ratio are exceptionally H-rich. MV Sgr, the hot R CrB star with a low C/He ratio, shows Balmer lines, but its H abundance has not been determined.

For HD 144941, the EHe star with the low C/He ratio and a hydrogen abundance $\log \epsilon$(H) $= 10.3$ (Harrison & Jeffery 1997), the measured H abundance offers a direct clue to the evolution. If the hydrogen represents a residue of original material that has not been exposed to H-burning, the *minimum* abundance for heavier elements is readily predicted from the solar abundances scaled to the H abundance. This assumes, of course, that the original material was approximately a solar mix of elements. The reported abundances for C to Fe are within 0.3 dex (i.e., the errors of measurement) equal to the adjusted solar values. There appear to be two extreme interpretations of this result. The low metallicity, of HD 144941 may be the initial metallicity, but this is weakly contradicted by the relative abundances that do not show the enhanced Mg/Fe and Si/Fe ratios expected of such a metal-poor star. Alternatively, if the hydrogen was accompanied by a solar mix of elements, the He-rich material with which it mixed was very metal-poor. It is also the case, as noted by Harrison & Jeffery, that not only is the C abundance low but there is also no indication of the N enrichment expected for He-rich material. We suggest that H-rich material of solar metallicity was mixed with He-rich material that had experienced gravitational settling of heavier elements.

For all but one of the other stars (including V652 Her), the measured Fe/H ratio is 2 or more orders of magnitudes greater than the solar ratio; no useful information is thus provided by the H abundance about the metallicity. DY Cen is a curious exception. It is relatively H-rich (Table 4). If this hydrogen is unburnt material of solar composition, the Fe abundance expected is $\log \epsilon$(Fe) $= 6.3$. If the hydrogen in this material has been partially consumed, this is a lower bound to the expected Fe abundance. The measured Fe abundance is 1.3 dex below this limit, indicating that either the star was initially metal-poor by at least 1.3 dex or the H-rich material has a peculiar composition. Jeffery & Heber (1993) did comment on dust–gas separation. Unlike the case of HD 144941, other elements do not mirror Fe. In fact, the measured abundances for elements other than Fe exceed the H-adjusted abundances by 0.6 dex or more, or, as shown in Fig. 12, the S/Fe and Si/Fe ratios are extraordinarily high. V854 Cen (Table 4) may present a milder form of the puzzle offered by DY Cen.

6.4 Nitrogen and oxygen

These elements with carbon provide the principal record of the nucleosynthesis and evolution that produced these H-poor stars. Nitrogen enrichment is the signature of H-burning CNO-cycled products. Carbon is most probably the leading product of He-burning. Oxygen and neon may accompany the carbon. Although one might suppose H-burning products to enter the atmosphere before the He-burning products, one should consider the possibility that nuclear processing may continue after the two products have mixed; possibly, H-burning continues or resumes after He-burning products enter the envelope. One hopes that the C, N and O abundances will reveal what happened. Normally, one would consider ratios N/Fe and O/Fe to be more accurate reflections of the N and O changes, because not only are certain errors minimized when using an abundance ratio but also the ratios allow for the changes of initial N and O abundance with initial Fe abundance. However, in Section 6.2 we suggested that the high Si/Fe and S/Fe ratios of key stars implied a depletion of Fe, and suggested using the mean of Si and S abundances.
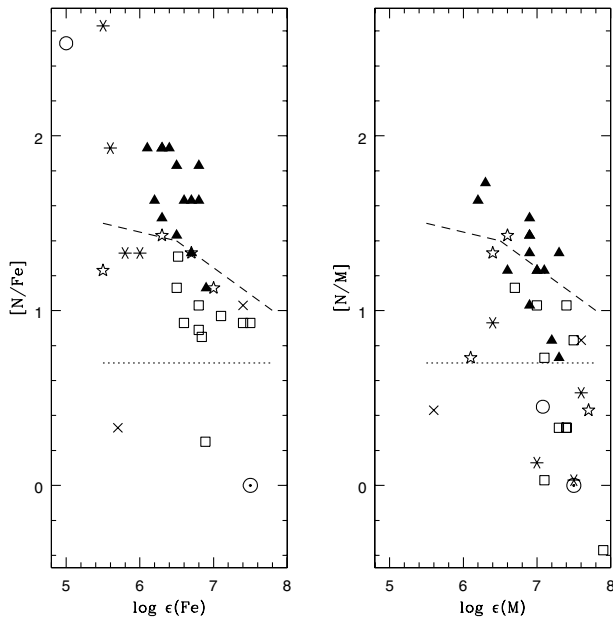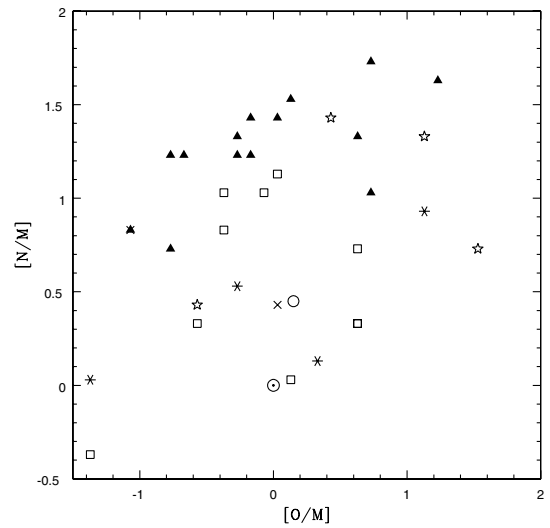
Figure 14. [N/Fe] versus log ϵ(Fe) and [N/M] versus log ϵ(M) for cool EHes, majority and minority class R CrB stars and hot EHes: Symbols: ☆ represent cool EHes, □ hot EHes, ▲ majority class R CrB stars, * minority class R CrB stars, ○ DY Cen, and × hot EHes with low C/He (~0.003 per cent). The Sun is denoted by ⊙. The dotted line represents conversion of the initial sum of C and N to N. The dashed line represents the locus of the sum of initial C, N and O converted to N.

If N-enrichment is due solely to the CN-cycle, the resultant N abundance is effectively the sum of the initial C and N abundances; the C/N ratio at equilibrium for the CN-cycle is small. In the event that the ON-cycle has acted, the N abundance is effectively the sum of the initial C, N and O abundances; the O/N ratio at equilibrium is small. Then, to interpret the N abundances, we need the initial C, N and O abundances as a function of metallicity.

The assumed initial C and O abundances are taken from Carretta, Gratton & Sneden (2000), i.e., [C/Fe] = 0 and [O/Fe] = +0.5 for [Fe/H] < −1, with a linear transition to this value from [O/Fe] = 0 at [Fe/H] = 0. Additionally, we take [N/Fe] = 0, but this is not a critical choice in view of the larger abundances of C and especially O. With these initial abundances, conversion of C to N, and C and O to N leads to the predicted trends shown in both panels of Fig. 14. Presently, there is a debate over the true initial O abundances. Analyses of ultraviolet OH lines (Israelian et al. 1998; Boesgaard et al. 1999) show [O/Fe] to increase linearly with decreasing [Fe/H], attaining [O/Fe] = +0.8 at [Fe/H] = −2.0 or log ϵ(Fe) = 5.5, the limiting inferred initial metallicity of our sample. If the OH-based trend were correct, conversion of C and O to N at low metallicity continues the upward trend shown in Fig. 14 for metallicities greater than log ϵ(Fe or M) = 5.5. Evidence is accumulating, however, that the high [O/Fe] values are probably overestimated (Asplund 2000; King 2000; Lambert 2000; Nissen, Primas & Asplund 2000; Asplund & García Pérez 2001).

Observed N and Fe or M (from Si and S) abundances are compared in Fig. 14 with the predictions for CN- and ON-cycling based on the initial C, N and O abundances. The key points that may be made include the following where, unless indicated otherwise, M (not Fe) is assumed to provide the initial C, N and O mix.

First, the majority R CrB stars have a maximum N abundance equal to that predicted from conversion of initial C and O to N. The

few exceptions have a N abundance between that predicted from conversion of C to N, and C and O to N. The Fe abundance implies lower initial C, N and O such that the observed N abundances of most R CrB stars exceed the prediction for conversion of initial C and O to N.
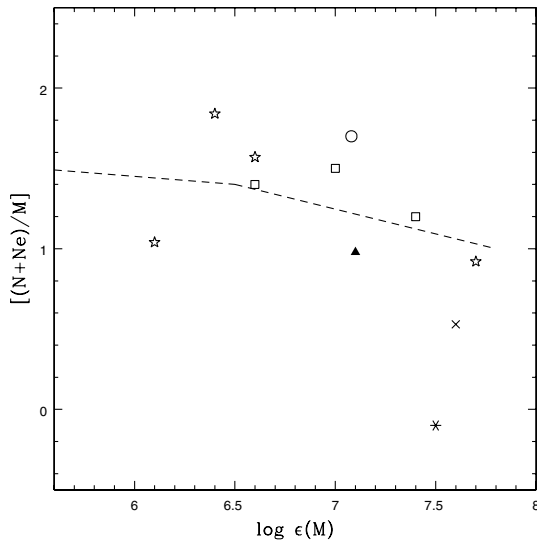
Second, the N abundances of the EHes are generally clustered between the predictions for N from CN- and ON-cycling, and appear to form an extension of the trend presented by the majority R CrB stars. Adoption of Fe as the metallicity indicator compresses the distribution of R CrB stars and EHes. Consistent with the idea that the N is a product of H-burning is the fact (Section 6.3) that the H abundance of the R CrB stars is on average less than that of the EHes.

Third, just three stars fall significantly off the N/M versus M trend, with a lower M than suggested by their N/M ratio: the minority R CrB VZ Sgr, the cool EHe star FQ Aqr, and the low C/He EHe star HD 144941. These stars provide the impression that there may be a distinct subclass of He-rich stars.

Fourth, although the N abundances imply wholesale conversion of O to N via the ON-cycle, many stars are not O-deficient (Fig. 15). Operation of the CNO-cycles reduces the C and O abundances. Obviously, the high C abundance of the R CrB stars and EHes implies C production from He-burning. At ON-cycle equilibrium, the O abundance is about 1 dex at 20 million K to 2 dex at 50 million K below its initial value. In a few R CrB stars and EHes the observed O abundance is 1 dex below the inferred initial abundance. In other stars the O abundance may be as much 1 dex overabundant relative to the initial abundance. This implies (see below) that O was synthesized along with the C, i.e., the 3α-process was followed by ^{12}C(α, γ)^{16}O. The most O-rich stars have an observed O/C ratio of near unity, implying roughly equal production of the two elements from He-burning.

6.5 Neon

Neon abundances are known for four hot EHes including the low C/He star V652 Her, the four cool EHes, DY Cen, the minority R CrB star V3795 Sgr, and the majority R CrB star Y Mus. In all but

Figure 15. [N/M] versus [O/M] for cool EHe, majority and minority class R CrB stars and hot EHes: Symbols: ☆ represent cool EHes, □ hot EHes, ▲ majority class R CrB stars, * minority class R CrB stars, ○ DY Cen, and × hot EHes with low C/He (~0.003 per cent). The Sun is denoted by ⊙.

Figure 16. [(N+Ne)/M] versus $\log \epsilon(M)$ for cool EHes, majority and minority class R CrB stars and hot EHes: Symbols: ☆ represent cool EHes, □ hot EHes, ▲ majority class R CrB stars, * minority class R CrB stars, ○ DY Cen, and × V652 Her with low C/He ($\sim$0.003 per cent). The dashed line represents the locus of the sum of initial C, N and O converted to N.

two stars neon is overabundant ([Ne/M] > 0). The two stars of low Ne abundance could be claimed to be unrepresentative of the family: V652 Her has a low C/He ratio for an EHe star, and V3795 Sgr is a 'peculiar' R CrB. In the remaining stars, neon is grossly overabundant: [Ne/M] $\sim$ 1–2.

Except for the hottest stars, the Ne abundances are based on Ne I lines in the red. Although the atmospheres are different, we recall that Auer & Mihalas (1973), in a classic paper on non-LTE effects, found LTE Ne abundances to be about 0.7 dex greater than the non-LTE, abundances for normal (i.e., H-rich) B stars with $T_{\rm eff}$ of 15000 to 22500 K and $\log g = 3$ to 4. If similar effects are present for this sample of He-rich stars, our Ne abundances are overestimated. In the hottest EHes, Ne II lines in the blue provide the Ne abundance (Jeffery 1996).

Here we shall assume that Ne is substantially overabundant in at least some of the EHes because it has been synthesized and added to the atmosphere. Synthesis could have occurred from exposure of CNO-cycled material to temperatures somewhat less than those required for He-burning. In such circumstances, ^{14}N through two successive α-captures is converted to ^{22}Ne. In He-burning at temperatures above about 250×10^6 K, ^{22}Ne$(\alpha,\rm n)^{25}$Mg destroys the Ne and serves as a neutron source. An instructive way to examine the data is to compare the sum of the N and Ne abundances as a function of the initial metallicity, as in Fig. 16.

In this figure the sum of the N and Ne abundances is shown relative to the predicted N abundance resulting from thorough conversion of initial C and O to N. The upper envelope of the points matches the predicted trend well. This result suggests an explanation for the generally lower N abundances of the EHes relative to the R CrB stars: the two groups experienced severe CNO-cycling resulting in conversion of initial C and O to N. However, in the case of the EHes, substantial amounts of the synthesized N was exposed to hot αs and converted to Ne. It will be necessary to extend the Ne measurements to the R CrB stars in order to show that Ne is not overabundant in them, a difficult task given the lower temperatures of the stars.

In principle, Ne (^{20}Ne) may also be made by an extension of

He-burning by α-capture on ^{16}O at high temperatures. Since the two modes of Ne synthesis produce different isotopes, we note the possibility of measuring the isotopic ratio. Odintsov (1965) measured the ^{22}Ne $- ^{20}$Ne shifts for a selection of red Ne I lines, finding values from 0.015 to 0.038 cm^{-1}. Since a shift of 0.038 cm^{-1} for a typical line is equivalent to a velocity shift of only 0.7 km s^{-1}, characterization of the isotopic mix will be difficult even from high-resolution, high-S/N spectra of the sharpest-lined stars.

6.6 Sodium to calcium

There are useful data on abundances in both the EHe and R CrB samples on Al, Si and S. Data on P and Ar are effectively available only for the EHes, on Ca for a few EHes but all R CrB stars, and Na only for the R CrB stars.

The Al/S ratios are close to the solar ratio, and uniform across the cool and hot EHes and majority R CrB stars. One EHe star stands out with a low Al/S ratio: BD $-9° 4395$, the star with emission lines: a subsolar Al and suprasolar S abundance combine to give a Al/S ratio of -2.3 dex compared to the solar ratio of -0.8 dex. HD 168476 appears to have a high Al/S ratio: Al/S = 0.2 dex, an uncertain value from Walker & Schönberner (1981) and much above the value of -1.0 from Hill (1965). Neither discrepant value deserves great weight at this time. Excluding these values, the mean abundance ratio of Al/S is -1.1 ± 0.3 dex from eight EHes, which compares well with the mean of -1.1 ± 0.2 dex from 12 majority R CrB stars. The cool EHes appear to have a similar Al/S ratio. The hint that the stellar ratios are less than the solar value of -0.8 dex is compatible with a slightly subsolar initial metallicity for the He-rich stars. There is a hint too that the ratios may differ from the solar ratio of -0.8 dex in the three minority R CrB stars but not in V854 Cen; Al is underabundant relative to S by about 1 dex.

The P/S ratio is solar within the measurement errors for the EHes: the mean P/S ratio is -1.4 ± 0.4 and -1.8 ± 0.3 dex, for the hot and cool EHes, respectively. Three hot EHes are suspected of a higher P abundance: HD 168476, LSE 78 and LS IV $+6° 002$, which are P-rich by 0.7 to 1.0 dex relative to the solar P/S ratio. For the cool EHe's BD $-1° 3438$, and LS IV $-1° 002$, the P/S ratio is normal. Among the R CrB stars (Asplund et al. 2000), phosphorus was measured in Y Mus (a majority R CrB star) and V3795 Sgr (a minority R CrB star), and reported to be overabundant by about 1 dex. Additional spectroscopic scrutiny is needed before a conclusion is reached concerning P in R CrB stars.

Argon abundances for seven hot EHes give a mean Ar/S ratio of -0.7 ± 0.1 dex, i.e., the solar ratio. The only other measurement for our He-rich stars is for the hot R CrB star DY Cen which has Ar/S = -1.0 dex, i.e., solar within the measurement errors.

Calcium in four of the five hot EHes in which it has been measured is of normal abundance: $\log [\epsilon(\rm Ca)/\epsilon(\rm S)] \simeq -0.9$, i.e., the ratio expected for solar-like and metal-poor stars. The exception is HD 168476, for which Walker & Schönberner (1981) give Ca and S of equal abundance. Of the four cool EHes, two have the Ca/S (and/or Ca/Si) ratio close to normal ratio. The other two, FQ Aqr and LS IV $-14° 109$, have Ca/S (and Ca/Si) about 1 dex below normal. Among the majority R CrB stars, the Ca/S ratio is 0.6 below normal with very little star-to-star scatter. Among the minority R CrB stars the Ca/S ratio is lower by about an additional 0.6 dex and similar to those of FQ Aqr and LS IV $-14° 109$. One interpretation of these in Ca/S and Ca/Si ratios is that they reflect systematic errors that vary from hot to cool stars. Another

speculation is that the low Ca abundance is a signature of alteration of the compositions by a process such as the winnowing of dust from gas.

Sodium abundances are unknown for the hot EHes. In the cool EHes, the Na/S ratio is solar or slightly higher, but the higher abundances are in part or in whole based on a strong line in a region rich in telluric H_2O lines. We give low weight to these results. In the majority R CrB stars, the Na/S ratio is normal (i.e., solar) at -0.8 ± 0.3 dex.

6.7 Heavy elements – Y and Zr

Our chief interest in the heavy elements is as tracers of exposure to the *s*-process. Unfortunately, heavy elements such as Y and Ba are difficult to detect in the spectra of the EHes. Therefore our data are restricted to the R CrB stars and a couple of the cool EHes. We
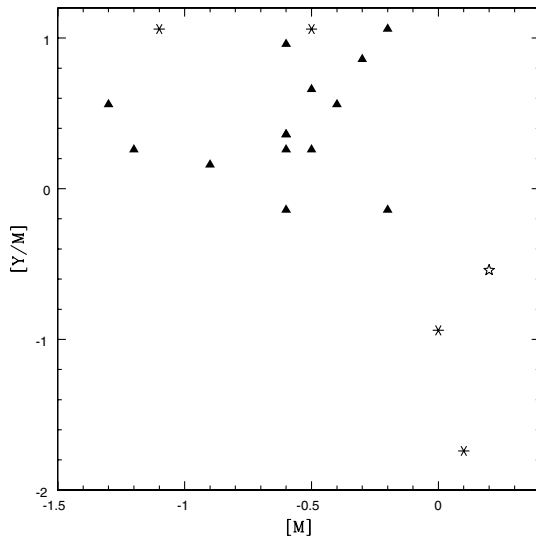
Figure 17. [Y/M] versus [M] for cool EHes, majority class R CrB stars and minority class R CrB stars: Symbols: ☆ represent cool EHes, ▲ majority class R CrB stars, and * minority class R CrB stars.
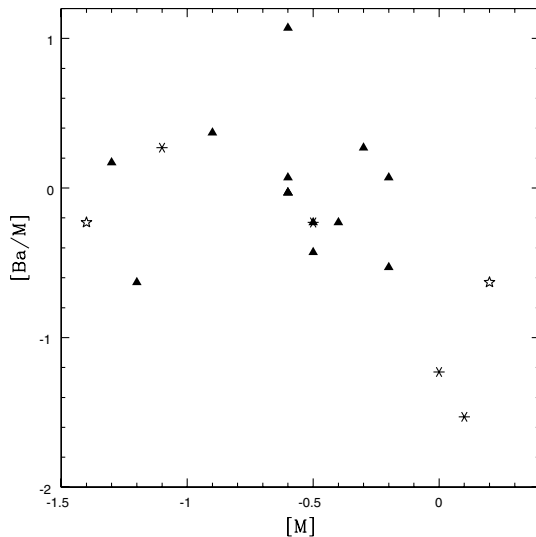
Figure 18. [Ba/M] versus [M] for cool EHes, majority class R CrB stars and minority class R CrB stars: Symbols: ☆ represent cool EHes, ▲ majority class R CrB stars, and * minority class R CrB stars.

emphasize the data for Y and Ba, but Sr was measured for all cool EHes and Zr and La in some cool EHes, and R CrB stars. To within the errors of measurement, the Sr/Y, Zr/Y and La/Ba ratios are as expected for normal stars.

The abundance of Y and Ba expressed as [Y/M] and [Ba/M] versus [M] show a scatter at a given [M] (Figs 17 and 18). The mean [Y/M] is slightly positive, but [Ba/M] scatters about zero. The lighter *s*-process elements seem enhanced relative to the heavy *s*-process elements. This mild (Y) to undetectable (Ba) *s*-process enrichment is at odds with an identification of the stars as remnants of H-rich thermally pulsing AGB stars. For example, Ba stars typically show enhancements of 0.8 to 1.6 dex, with a slight increase in the Ba to Y ratio with decreasing metallicity. If He-rich stars were previously on the AGB, they did not experience the third dredge-up.

These conclusions, based primarily on *s*-process abundances measured for the R CrB stars, are dependent on identifcation of M (not Fe) as the initial metallicity. If Fe is chosen in preference to the Si-S abundances, Y/Fe and Ba/Fe indicate a modest *s*-process enrichment in the R CrB stars.

7 A SIMPLE RECIPE AND APPLICATION

7.1 Recipe

The overall impression gained from the inspection of the spectra and confirmed by the abundance analyses is that the atmosphere of a H-deficient star most likely consists of three ingredients: a small fraction of H-rich material with original elemental abundance ratios (except, perhaps, for some conversion of C to N), a large fraction of severely H-depleted He-rich material, and a fraction of material from a He-burning layer. The three layers may not necessarily have belonged to a single star. The principal tracers of the three layers are H, N, and C with O, respectively. Our simplest recipe assumes that there was no processing after mixing of ingredients. In particular, we assume that the C-rich material from the He-burning layer was not subsequently exposed to H-burning CN-cycling. If we take the metallicity M derived from the mean of Si and S, the maximum observed N abundance may be accounted for without a call for CN-cycling of the C-rich material from the He-burnt layer.

Perhaps, the single most striking aspect of the EHes is the near-uniformity of their C/He ratios. For all except HD 144941 and V652 Her, the ratio is in the narrow range $0.3-1.0$ per cent, a range not much greater than that expected from errors of measurement. The C/He ratio of R CrB stars is not directly measurable. The hot R CrB star DY Cen has a ratio matching that of the majority EHes, but MV Sgr has a much lower ratio. In its simplest form, our recipe provides He from H-burnt material, but C only from the He-burnt material (in the exceptional case of HD 144941, the surviving H is accompanied by a significant amount of carbon). The observed C/He ratio, then, results from a mixing of a mass of H-burnt material M_{CN} with mass fractions $f_{CN}(He) \simeq 1$ and $f_{CN}(C) \simeq 0$, and a mass of He-burnt material $M_{3\alpha}$ with mass fractions $f_{3\alpha}(He)$, $f_{3\alpha}(C)$ and $f_{3\alpha}(O)$ for He, C and O, respectively, where $f_{3\alpha}(He) + f_{3\alpha}(C) + f_{3\alpha}(O) = 1$. If $m_{mix} = M_{3\alpha}/M_{CN}$, the C to He ratio is given by

$$\frac{Z(C)}{Z(He)} = \frac{f_{3\alpha}(C)m_{mix}}{1 + f_{3\alpha}(He)m_{mix}}, \tag{3}$$

where $Z(X)$ is the mass fraction of element X in the mixed envelope.

The near-uniformity of the C/He ratios allows for several possibilities. Suppose He-burning ended far from completion: $f_{3\alpha}(\text{He}) \simeq 1$ with $f_{3\alpha}(\text{C}) \ll 1$. If, then, $m_{\text{mix}} \gg 1$, the observed C/He ratio is given by $Z(\text{C})/Z(\text{He}) \simeq f_{3\alpha}(\text{C})$. This demands that all stars run He-burning to very similar and incomplete levels. Alternatively, He-burning ran to near-completion with $f_{3\alpha}(\text{C}) \simeq 1$ [or, more properly, $f_{3\alpha}(\text{C}) + f_{3\alpha}(\text{O}) \simeq 1$ with similar mixes of C and O, and even Ne in some cases]. Now, $Z(\text{C})/Z(\text{He}) \simeq f_{3\alpha}(\text{C})m_{\text{mix}}$ with $m_{\text{mix}} \ll 1$, which seems a more palatable recipe in that moderate variations of $f_{3\alpha}(\text{C})$ occasioned by temperatures and the time-scale of He-burning are allowed. It remains, however, unclear what constrains the mixing fraction to small values. Oxygen production depends not only on the rate constant for $^{12}\text{C}(\alpha, \gamma)^{16}\text{O}$ but also on the time-scale (and temperature) for He-burning. If He is consumed quickly by the 3α-process, ^{12}C is the principal product, but if He is consumed slowly, ^{12}C may be converted to ^{16}O. This means that the envelope's C/O ratio offers insight into how helium was burnt.

In our recipe, the surface C abundance is not directly dependent on the star's initial composition. This independence does not apply to N and O. Fortunately, initial C, N and O abundances may be inferred (see above). Nitrogen according to the recipe is contributed by the H-burnt material only. If H-burning is due to the CN- and ON-cycle,

$$Z(\text{N}) = \frac{Z(\text{C} + \text{N} + \text{O})_0}{1 + m_{\text{mix}}}, \qquad (4)$$

which, if $m_{\text{mix}} \ll 1$, implies $Z(\text{N}) \simeq Z(\text{C} + \text{N} + \text{O})_0$, where the subscript 0 denotes the star's initial composition. If CN-cycling alone operates, $Z(\text{N}) \simeq Z(\text{C} + \text{N})_0$.

According to our recipe, the O abundance in the limit that O is converted to N by ON-cycling and $m_{\text{mix}} \ll 1$ is given by

$$Z(\text{O}) \simeq \frac{f_{3\alpha}(\text{O})m_{\text{mix}}}{1 + m_{\text{mix}}}. \qquad (5)$$

ON-cycling is a slower process than CN-cycling. Calculations (Arnould, Goriely & Jorissen 1999) show, however, that steady H-burning results in a substantial reduction of O before H is completely converted to He by the CN-cycle. This result, applicable to a solar ratio of C, N and O to H, will hold for reduced abundances of the catalysts. Establishment of the low O/N (~ 0.1) equilibrium ratio occurs for H deficiencies of about 1 to 1.5 dex and greater for temperatures of 25 to 55 million K. At temperatures of 15 million K and less, consumption of O is too slow and CN-cycling exhausts the H supply before O is depleted. By contrast, CN-cycle participants are close to their equilibrium abundances after consumption of just a few protons per catalyst, that is a reduction of the H mass fraction by a mere 0.0004 from its initial value of about 0.75. These equilibrium abundances persist as the ON-cycle participants attain equilibrium. If CNO-cycling is the sole nuclear activity at temperatures of greater than about 25 million K, one expects reduced C and O and enhanced N abundances in material that is H-depleted by about 1 dex or more, but a reduction restricted to the C abundance alone in material that is H-depleted by *less* than about 1 dex. Given that the typical H-deficiency of the EHes and R CrB stars (Table 3) is 4 or more dex, O deficiencies (Fig. 15) are expected unless H-burning occurred at or below 15 million degrees K. At ON-cycle equilibrium, the O abundance is about 1 dex at 20 million K to 2 dex at 50 million K below its value, assuming solar ratios, and the

N abundance is greater than the surviving O abundance by corresponding amounts.

Inspection of Fig. 15 shows that the minimum O abundance is indeed about 1 dex below the initial value. The N abundance for these stars is about 1.5 dex greater than the O abundance, in fair agreement with CNO-cycle expectation. Oxygen-deficient stars are, however, a minority among our stars. EHes do not show the high N abundance expected of O-deficient material. Formally, our recipe allows for a reduced N abundance (relative to that from CNO-cycling) by increasing m_{mix} in equation (4), but a large value of m_{mix} implies $Z(\text{O}) \simeq f_{3\alpha}(\text{O})$ and, in all probability, an O abundance much greater than the observed range [O/M] of -1 to $+1.5$. Thus we do not favour this alternative. A possible explanation is that the H-poor, He-rich material added to the envelopes resulted from H-burning at temperatures of about 15 million K or less, at which the ON-cycle is very slow. This would preserve the O abundance, but would not account for the large spread in the O abundances (Fig. 15), which would seem to call for addition of O from He-burning. The more likely explanation suggested by the Ne abundances is that substantial amounts of N have been converted to ^{22}Ne.

Before proceeding further, we recall the carbon problem presented by the R CrB stars. Our conclusion about the greater degree of ON-cycled material in R CrB stars is dependent on the relative abundances of C, N and O, and the metallicity [M]. Recall that [M] generated from the mean of Si and S abundances was chosen because Fe (also Ca and Ti) appears depleted, especially for the R CrB stars and quite apparently so for the minority R CrB stars. What if [M] itself is not a fair indicator of the initial metallicity of the R CrB stars? For example, if [M] were increased by 0.5 dex on average, the predicted N abundances following CN-cycling would be similarly increased and would match the observed N abundances. Initial O abundances would be similarly increased by about 0.5 dex above the observed O abundances. Now, an explanation not involving conversion of O to N must be found for the O underabundances. What is needed, if CN-cycling alone is to account for the atmospheric compositions of R CrB stars, is a reduction of the N abundances for almost all stars, and an increase of the O abundances for at least the O-poor stars. This is an unlikely combination, given the similarity of the dependence of the N I and O I lines to the atmospheric parameters. Indeed, most of the proposed solutions to the carbon problem effectively preserved elemental abundance ratios such as O/N (Asplund et al. 2000). We suggest that it is likely that the R CrB atmospheres are substantially contaminated with ON-cycled material.

7.2 Application

Dissection of the compositions of the majority R CrB stars is summarized in Table 6, where stars are ordered by the difference between the observed and predicted O abundances (Δ in Table 6). The observed N abundance is listed, followed by the predicted abundance assuming first that initial C is converted to N, and second that initial O is also converted to N. Throughout the sample, with the possible exception of RY Sgr, the observed N abundances exceed the former prediction: the mean excess is 0.5 ± 0.2 dex. In contrast, the observed N abundances match the latter prediction: the mean difference is 0.0 ± 0.2 dex for all 14 stars. In our interpretation, material present in these atmospheres is only heavily CN- and ON-cycled before He-burnt material was added without subsequent exposure to hot protons.

The O/C ratio of the He-burnt material which is estimated from

Table 6. Predicted and observed compositions of majority R CrB stars, where stars are ordered by the difference between the observed and predicted oxygen abundances.

	[M]	$\log \epsilon(O)_{obs}$	Δ^c	$\log \epsilon(N)_{obs}$	$\log \epsilon(N)_{predicted}$		$\log \epsilon(C)_{obs}$	O/C
					$\log \epsilon(C+N)_0$	$\log \epsilon(C+N+O)_0$		(He-burnt)
UV Cas[a]	−0.3	7.5	−1.1	8.5	8.4	8.8	9.2	0.02
Y Mus	−0.4	7.7	−0.9	8.8	8.4	8.8	8.9	0.06
FH Sct	−0.5	7.7	−0.8	8.7	8.3	8.7	8.8	0.08
RY Sgr[a]	−0.2	7.9	−0.8	8.5	8.6	8.9	8.9	0.10
UW Cen	−0.9	7.7	−0.6	8.3	7.9	8.5	8.6	0.13
V482 Cyg	−0.6	8.1	−0.4	8.8	8.2	8.7	8.9	0.15
GU Sgr	−0.5	8.2	−0.4	8.7	8.3	8.8	8.8	0.25
RT Nor	−0.2	8.4	−0.3	9.1	8.6	8.9	8.9	0.30
RS Tel	−0.6	8.3	−0.1	8.8	8.2	8.6	8.9	0.30
XX Cam[b]	−0.6	8.4	0.0	8.9	8.2	8.6	9.0	0.30
SU Tau	−1.2	8.4	0.3	8.5	7.7	8.3	8.8	0.40
R CrB[b]	−0.6	9.0	0.5	8.4	8.2	8.7	9.2	0.60
RZ Nor	−0.6	8.9	0.5	8.7	8.1	8.6	8.9	1.00
UX Ant	−1.3	8.8	0.8	8.3	7.6	8.2	8.9	0.80

[a] Incomplete CN-cycling?
[b] CN-cycling of fresh C?
[c] $\Delta = \log[\epsilon(O)_{obs}/\epsilon(O)_0]$.

Table 7. Predicted and observed compositions of EHes, where stars are ordered by the difference between the observed and predicted oxygen abundances.

	[M]	$\log \epsilon(O)_{obs}$	Δ^f	$\log \epsilon(N)_{obs}$	$\log \epsilon(N)_{predicted}$		$\log \epsilon(C)_{obs}$	O/C
					$\log \epsilon(C+N)_0$	$\log \epsilon(C+N+O)_0$		(He-burnt)
BD−9°4395[a]	0.4	7.9	−1.4	8.0	9.1	9.5	9.10	0.05
BD+10°2179[b]	−0.2	8.1	−0.6	8.1	8.6	8.9	9.50	0.04
LS IV−14°109[e]	0.2	8.5	−0.6	8.6	8.9	9.3	9.45	0.10
HD 124448	0.0	8.5	−0.4	8.8	8.7	9.1	9.50	0.10
HD 168476	−0.1	8.4	−0.4	8.9	8.7	9.0	9.50	0.10
LSS 3184	−0.8	8.1	−0.3	8.3	8.0	8.5	9.00	0.10
LS IV +6°002	−0.5	8.3	−0.2	8.5	8.3	8.7	9.40	0.10
LSS 99[c]	−0.4	8.6	0.0	7.6	8.4	8.8	9.10	0.30
BD−1°3438	−0.9	8.4	0.1	8.5	7.9	8.5	8.90	0.30
LSE 78	−0.4	9.1	0.5	8.3	8.4	8.8	9.50	0.20
LS II +33°005[d]	−0.1	9.4	0.6	8.2	8.6	9.0	9.40	0.70
LSS 4357[d]	−0.1	9.4	0.6	8.2	8.6	9.0	9.40	0.80
LS IV−1°002	−1.1	8.9	0.8	8.2	7.8	8.3	9.30	0.30
FQ Aqr	−1.4	9.0	1.2	7.3	7.5	8.0	9.20	0.60

[a] Star has a non-solar mix of metals. At [M] = 0.4, which seems extraordinarily high, the observed N is less than the initial N. If Fe taken as initial metallicity ([M] = −0.9), N is consistent with CN-cycling prediction.
[b] N is less than predicted by CN-cycling of initial C. Non-solar mix of metals. If Fe taken as initial metallicity ([M] = −1.0), N implies CN- and some ON-cycling.
[c] No CN-cycling! Observed O very similar to inferred initial O, and therefore the O/C ratio of He-burnt material is very low.
[d] Observed N less than expected from CN-cycling. [M] too high?
[e] N abundance too low to account for the low O abundance.
[f] $\Delta = \log[\epsilon(O)_{obs}/\epsilon(O)_0]$.

the observed O and C abundances might be regarded as an upper limit, because we do not correct for surviving initial O, and also the C abundance used is the spectroscopic C abundance, which is always lower than the input C abundance for R CrB stars. The O/C ratio ranges from negligible to substantial, a range that may be incompatible with assumptions behind our simple recipe.

Results for the hot and cool EHes (Table 7) present a different picture. For five stars the observed N abundance is appreciably (0.4 dex or more) less than that predicted from conversion of initial C to N. Except in two cases (BD −1° 3438 and LS IV −1° 002), the N abundance can be accounted for without demanding ON-cycled material be now present in the atmospheres. Recall that the available Ne abundances imply that the lower N abundances of the EHes may be due to partial conversion of N to ^{22}Ne at temperatures just too cool for He-burning. BD −9°4395, whose spectrum shows

emission lines, is the only star in Table 7 with observed N less than the initial N; adoption of Fe as M, however, eliminates this problem. The inferred O/C ratios for the He-burnt material span the range inferred from the majority R CrB stars. Note that V652 Her and HD 144941 with low C/He (~0.003 per cent) are not included in Table 7.

The N abundances of the R CrB stars show that their atmospheres are substantially contaminated by ON-cycled, as well as CN-cycled material. The EHes have a lower N abundance that does not directly imply substantial ON-cycling. When neon abundances are included in the picture, it is seen that the sum of the N and Ne abundances is equivalent to the N anticipated from the combination of CN- and ON-cycling; the N was apparently converted to ^{22}Ne by α-captures prior to ignition of He. This difference between EHes and R CrB stars has important

consequences for the understanding of the evolution of these H-poor stars. Understanding can be deemed complete only when the links, if any, between EHes and R CrB stars are identified, and the progenitors and descendants of the stars are identified. At present, the progenitors are unknown. Two scenarios are discussed in Section 9. Here, we ask – do EHes evolve into R CrB stars? Or do R CrB stars evolve into EHes? Or do the two classes have different origins? It is possible that the answer is 'Yes' to all three questions for subsets of the stars.

Consider the case of evolution of EHes to R CrB stars. He-burning products are present in the EHes such that C/He is uniform from one EHe to another with a couple of exceptions. Given that C/N ~10 for the EHes and that a factor of about 3 enrichment of N is needed to produce a R CrB, a relatively mild processing of C to N is called for to turn a EHe star into a R CrB star. This call for processing and mixing is reminiscent of the first dredge-up in normal low-mass red giants. Noting that the O abundances of the two kinds of stars are similar, CN-cycling must suffice for the production of additional N, a requirement calling for low-temperature H-burning. This picture must meet one additional constraint: the EHes must contain an adequate supply of protons to sustain conversion of C to N. Since the N abundance must be

increased from about $\log \epsilon(N) \sim 8$ to 8.6 and each conversion requires a minimum of two protons, the initial H abundance should exceed 8.8. This is close to the maximum value seen in EHes. There is a rough anticorrelation between high H abundance and low N abundance among EHes. Additionally, the R CrB stars as a class have lower H abundances than the EHes, and too little H to sustain significant additional conversion of C and O to N. The R CrB stars should have a lower C/He ratio than the EHes. This prediction can not be excluded. Evolution of EHes to R CrB stars requires the R CrB stars to have the high Ne abundances seen in the EHes. The one measurement for a majority R CrB star just meets this requirement. Additional measurements of Ne in R CrB stars are now needed. However, a difficulty remains. In this scheme, the N abundance of the R CrB stars is the fruit of conversion of initial C and O to N, supplemented in a major way by conversion of fresh C to N. Then, the fact that their N abundances are close to the maximum expected from total conversion of initial C and O to N is an accident. This is, perhaps, the leading objection to the proposal that EHes evolve to R CrB stars with additional N production via conversion of fresh C to N. Adoption of Fe rather than Si and S are the indicators of a R CrB's metallicity removes this objection.

The uniform C/He ratio of the EHes, and the generally lower N
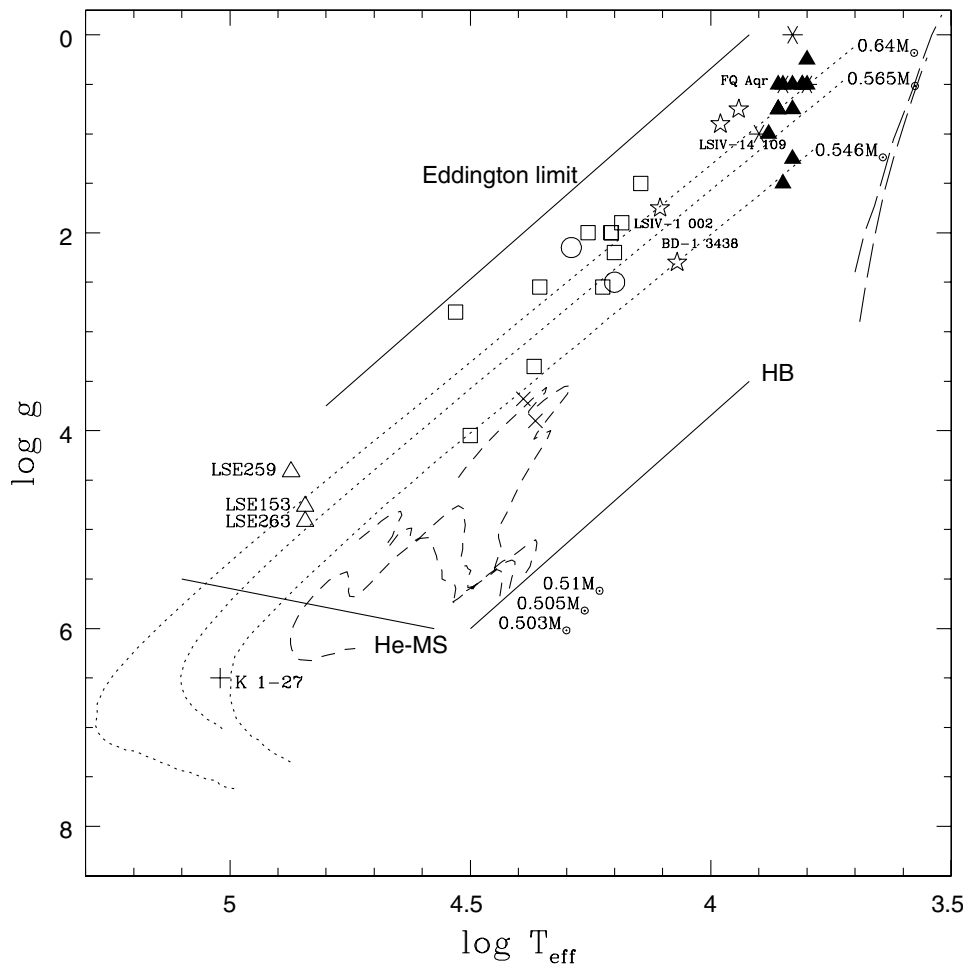
Figure 19. $\log g - \log T_{eff}$ diagram for cool EHes, R CrB stars, hot EHes, HesdO stars, and O(He) stars: Symbols: ☆ represent cool EHes, ▲ majority class R CrB stars, * minority class R CrB stars, ○ hot R CrB stars, □ hot EHes, × hot EHes with low C/He (~0.003 per cent), △ HesdO stars, and +O(He) stars. Solid lines show the helium main-sequence, the horizontal branch and the Eddington limit for pure Thomson scattering in a helium atmosphere. Evolutionary tracks of post-AGB (Schönberner 1983), post-EHB (Caloi 1989), and RGB and AGB that begin from the HB (Giridhar et al. 2000) are shown by dotted, short dashed, and long dashed lines, respectively, for different masses.

of EHes are obstacles to accepting that evolution proceeds from the R CrB stars to the EHes. Although N can be reduced and Ne enhanced by deep mixing that adds material raised to or beyond the temperatures of He-burning, it seems likely that C is added at this time and a dispersion in C/He created. An astute reader will appreciate that the uniform C/He ratio is unexplained by us and simply assumed to result from formation of an EHe. Clearly, the uniformity unless it is an aberration of small-number statistics implies a narrow range of progenitors and a single mode of formation for EHes.

The third scenario considers the EHes and R CrB stars to differ from birth. Subsequent evolution may drive EHes to higher temperatures and R CrB stars to lower temperatures; for example, R CrB stars are likely evolve to higher $T_{\rm eff}$ and so appear among the EHes, but if the evolution is rapid relative to the lifetime of EHes formed directly, contamination of the EHe sample with evolved R CrB stars could be small. Despite differences in composition, there are considerable similarities between EHes and R CrB stars that suggest that they may have a common parentage.

There remain the minority R CrB stars, the hot R CrB star DY Cen, and the low C/He ratio hot EHes. A key problem with the minority R CrB stars is identification of their initial composition; Si and S (Table 4) imply modest deficiencies ([M] ∼ 0.1 to −0.4, except for V854 Cen) but iron (and other elements) indicate [Fe] ∼ −1.7 to −2.4. Given this distortion of elemental ratios, one wonders if C, N and O were immune. It probably suffices to comment on one star and allow the reader to check that the other stars will also not neatly fit our recipe. Consider V3795 Sgr for which [M] ∼ 0 but [Fe] = −1.9. The observed N abundance is solar (i.e., the presumed initial value) not the 0.7 dex greater value expected from CN-cycling. To compound the puzzle, O is depleted by 1.4 dex. Except for V854 Cen, the other three minority R CrB stars exhibit a similar problem. Nitrogen in V854 Cen implies substantial CNO-cycling and a O/C ratio of the He-burnt material of about 0.2. The peculiar abundance ratios such as Si/Fe and S/Fe are difficult to understand in terms of nucleosynthesis, except perhaps as a *rp*- (effectively *rα*-) process enriching α-nuclides up to Si and S but not Ca. Given the presence of post-AGB stars and RV Tauri variables with photospheres highly depleted in elements that condense easily into dust grains, one is tempted to invoke this process for the minority R CrB stars, and in a milder form for the majority R CrB stars; Asplund et al. (2000) discussed this idea. A difficulty is that hardy grains in C-rich environments are those of SiC yet Si is not depleted. Since the EHes as a class do not show highly anomalous Si/Fe and S/Fe ratios, we presume that the process operated in the R CrB stars themselves or in their progenitors. Certainly, extended atmospheres with a propensity to form dust are auspicious sites for winnowing of dust from gas. Binarity seems to encourage the winnowing in post-AGB stars and possibly the RV Tauri variables (Van Winckel, Waelkens & Waters 1995; Giridhar et al. 2000). Rao et al. (1999) speculated that R CrB may be a binary.

Finally, there are the two EHes with a low C/He ratio. HD 144941 was discussed in Section 6.3. V652 Her with [M] ≃ 0.1 seems to fit the picture of an atmosphere with considerable amounts of CN- and ON-cycled material. The low C abundance implies a small fraction of He-burnt material of indeterminate O/C ratio. The merger of two helium white dwarfs could result in formation of EHes with a low C/He ratio and lower luminosity (Saio & Jeffery 2000).

Our discussion assumes Ne to be a product of α-captures on N. Attribution of Ne overabundances to extended He-burning

seems questionable, because the Ne overabundances are found in stars with low O/C and high O/C from the 3α-processed material. High C and high Ne, at least in our simple view of the He-burning zone, are incompatible; the Ne-rich material is necessarily C-poor.

8 THE THEORETICAL HERTZSPRUNG–RUSSELL DIAGRAM

For comparisons with theoretical evolutionary tracks, it is convenient to consider observed and theoretical stars in the Kiel diagram of $\log g$ versus $\log T_{\rm eff}$, where stars are represented by observationally determined quantities. On the assumption that He-rich stars once created evolve continuously, different classes of the stars will appear connected in the HR diagram. Particularly rapid evolutionary phases connecting slower phases will probably appear as unpopulated gaps, especially given small sample sizes. In this diagram (Fig. 19), the hot EHes, cool EHes and the R CrB stars form a quasi-continuous sequence suggesting but not requiring an evolutionary link between them. The sequence is bounded by lines of constant L/M corresponding to $\log L/M$ ∼ 3.75 to 4.5; evolution from the AGB to the top of the white dwarf cooling track occurs at constant L. Also shown is the horizontal branch (HB), and the extreme horizontal branch (EHB) stars populate the very blue edge of HB (Fig. 19).

Before turning to theoretical ideas on how to populate the constant L/M strip with He-rich stars, we comment on putative relatives of the EHes and R CrB stars, i.e., stars at either end of the strip having compositions like those of the EHes and R CrB stars.

At the cool end are the cool hydrogen-deficient carbon stars (HdCs) which, according to the only analysis available, seem to be a close match to the R CrB stars (Warner 1967). Visible spectra of HdCs are replete with strong molecular lines that have proven a deterrent to quantitative analysis.

Beyond the hot end of the EHe sequence are stars variously classified as sdB, sdO including the central stars of planetary nebulae, and then the white dwarfs. He-rich stars are found throughout this hot extension. The sdO-sdB region is home to two kinds of stars. There are stars of low g that are called 'luminous' sdB or sdO stars, and at higher g are 'compact' sdB and sdO stars (Haas et al. 1996). The former are most probably post-AGB stars, and the latter post-EHB stars; sample post-AGB and post-EHB evolutionary tracks are shown in Fig. 19. Whether luminous or compact, the stars show a wide range in H abundance and include He-rich objects. In the observed sample of luminous stars are some that qualify as putative relatives, presumably descendants, of the EHes and R CrB stars.

Husfeld et al. (1989) analysed three stars (LSE153, LSE259 and LSE263) with $T_{\rm eff}$ ∼ 70 000 K and $\log g$ ≃ 4.7 with no detectable H: the limit H/He ≤ 5 to 10 per cent by number is not very restrictive, because the Balmer lines in these hot stars coincide with the Pickering lines of He II. For two stars, C/He ≃ 2 per cent, a value similar to that of the EHes, but a third star is C-poor with C/He ∼ 0.01 per cent. The N abundances are rather higher than found for EHes, but at the upper end of the range for R CrB stars. At higher effective temperatures, He-rich stars exist among central stars of planetary nebulae: e.g., the O(He) star in the planetary K 1−27 (Rauch, Köppen & Werner 1994) with $T_{\rm eff} = 10^5$ K and $\log g = 6.5$ has H/He ≤ 0.2, a N abundance slightly higher than that of an N-rich R CrB star but no detectable C or C/He ≤ 0.5 per cent. This qualifies as a R CrB descendant. One supposes that the sequence of He-rich star ends in the DO white dwarfs. Although the paucity of data cannot be overlooked, it does seem possible to

identify relatives of the EHe and R CrB stars between the hottest EHes and R CrB stars and the start of the white dwarf cooling track. Then, surface compositions may be altered by gravitational settling such that they lose their memory of their antecedents (Dreizler 1999).

There are other He-rich stars that, judged by T_{eff} and $\log g$, could be relatives of the EHes and the R CrB stars. These are the Wolf–Rayet [WC]-type central stars of planetary nebulae (CSPN) and the PG 1159 stars. The He-rich CSPN have $T_{eff} \sim$ 75 000 to 180 000 K and $\log g \simeq 5.5$ to 8.0. Their surface composition is typically He : C : O $\sim$ 1 : 0.5 : 0.1 by number (Leuenhagen & Hamann 1998), i.e., C and O are very much more abundant than in the EHes and the R CrB stars. PG 1159 stars have a similar composition. Dreizler & Heber's (1998) analyses of nine stars give mean number ratios: C/He = 0.3, O/He = 0.06 with very low N abundances (N/He $\leq 10^{-4}$ for non-pulsators and 0.01 for the pulsators). Helium-burning products are a more serious contaminant in these stars than in the EHes and R CrB stars. Evolution along a post-AGB track will not provide the necessary mixing. Therefore it appears that these C-rich stars and the EHe/R CrB stars originate in different ways.

9   EVOLUTIONARY SCENARIOS

Recent discussions of EHes and R CrB stars have focused on two theoretical proposals for their origins. The double-degenerate (DD) scenario invokes the merger of a He white dwarf with a C–O white dwarf. The final-flash (FF) scenario supposes a late or final He-shell flash in a post-AGB star that re-expands the star to giant dimensions. Asplund et al. (2000) provided a discussion of the DD and FF scenarios, and assessed their ability to account for the compositions of R CrB stars. In a few cases, notably the low C/He EHes V652 Her and HD 144941, a post-EHB origin may account for the stars.

Evolution off the AGB is very unlikely to produce a He-rich star such as HdC or a R CrB directly by loss of the H-rich envelope. A H-rich post-AGB star may experience subsequently a final He-shell flash, reconversion to an AGB-like star, destruction of hydrogen in its envelope, and a decline along a post-AGB track back to the white dwarf cooling track. Early discussions of the FF scenario are given by Fujimoto (1977), Schönberner (1979) and Iben & Renzini (1983). More detailed discussions by Herwig, Blöcker & Driebe (1999) and Herwig (1999) have shown how diversified the FF scenario may be.

There is a fundamental problem in identifying EHes and R CrB stars as post-AGB stars from an FF. The He-shell of an AGB star is rich in C and O with mass fractions (He $\sim$ C $\sim$ O) if convective overshoot is considered (Herwig 2000). Without overshoot the ratios are He : C : O $\approx$ 0.7 : 0.3 : 0.01 by mass fractions. The final He-shell flash cannot greatly modify this mixture, because the mass of the H-rich envelope is necessarily very small. The observed ratios are very different; for example, He accounts for more than 95 per cent of the He mass of an EHe. This sharp difference between the predicted and observed compositions suggests that the EHe-R CrB sample cannot be comprised of post-AGB stars. These post-AGB stars should also be rich in ^{13}C, but the ^{13}C abundance is low according to upper limits for R CrB stars. Absence of observed s-process enrichments also rules out an association with thermally pulsing AGB stars.

Herwig (1999) points out that the fate of a star evolving directly off the AGB depends in large part on how recently it experienced a He-shell flash or thermal pulse (TP). He identifies four principal possibilities.

(1) **No additional TP.** If the star departs soon after a TP, it is most likely to settle on the white dwarf track and not experience another TP. Such stars are not progenitors of EHes and R CrB stars.

(2) **A very late TP.** A more delayed departure from the AGB results in a return from the white dwarf cooling track to the domain of the EHes and R CrB stars. The H-rich envelope is engulfed by the He-burning layers of the TP. Although H is thoroughly depleted by the models, the problem is that He, C and O are produced with roughly equal mass fractions, and N is not produced in significant amounts. In addition, the depletion of hydrogen takes place by the reaction $^{12}C(p, \gamma)^{13}C(\alpha, n)^{16}O$. The produced neutrons are captured by Fe seed nuclei resulting in enrichment of s-process elements, but the s-process elements in R CrB stars and cool EHes are Sun-like, except for mild enhancement of light s-process elements for majority class R CrB stars.

Lithium is brought to the surface by dredge-up in a very late TP. The reaction $^3He(\alpha, \gamma)^7Be(e^+ \nu)^7Li$, produces ^7Li from ^3He. ^3He enters into He-flash convective zone during a very late TP, together with hydrogen from the envelope. Lithium is present only in four R CrB stars out of the 18 analysed R CrB stars (Asplund et al. 2000). The hot R CrB star MV Sgr shows Li in emission (Pandey, Rao & Lambert 1996).

(3) **A late TP.** An even more delayed departure from the AGB leads to a TP occurring before the H-burning shell has turned off. Subsequent evolution follows that of the VLTP except the envelope is not mixed into the He-shell, but dredge-up in the freshly renovated AGB star does subsequently reduce the surface H abundance. In contrast to the VLTP, the surface H abundance is reduced by a factor of only about 50. The final He, C and O (and N) surface mass fractions are also unlike the observed abundances of the EHes and the R CrB stars.

(4) **A very early TP.** Departure from the AGB immediately following a TP occurs when the envelope mass is very small, and a dredge-up commenced at this time reduces the H mass fraction by perhaps 20 per cent at most.

As argued by Schönberner (1996), the FF scenario cannot account for the EHes and R CrB stars with their low C/He ratio. There are stars that do match the predicted FF abundances quite well. In particular, a rare few have evidently evolved from a WD dwarf-like state to an AGB in a very short time, as the model predicts. Sakurai's object (V4334 Sgr) is probably experiencing a very late TP. Its surface composition evolved considerably over a few months before the photosphere was obscured by a thick cloud of dust (Asplund et al. 1997b, 1998, 1999). Herwig (1999) showed that rapid changes of surface composition are a feature of such a TP. Predicted changes resembled those observed. FG Sge is a second candidate for a late TP with presently characteristics of a R CrB. Despite these correspondences between observations and predictions of the FF scenario, identification of majority R CrB stars and EHes as fruits of the scenario is highly questionable. On the other hand, the FF scenario accounts well for the H-poor central stars of planetary nebulae and PG1159 stars with their mix of He $\sim$ C $\sim$ O.

The DD scenario exploits the fact that a small fraction of binary systems evolve to a pair of degenerate white dwarfs, for example, a He white dwarf orbiting a C–O white dwarf. Angular momentum losses via gravitational wave radiation or a magnetic field

interaction ultimately cause the merger of the stars: the He white dwarf is consumed by the C−O white dwarf. The merged star expands to red giant dimensions. This idea was put forward by Webbink (1984) and Iben & Tutukov (1985). Iben, Tutukov & Yungelson (1996) showed not only that this binary model can account for the observed number of R CrB stars and EHes in the Galaxy, but also mention several different production channels that might account for differences of composition. In this scenario, the coexistence of high abundances of C and N at the surface of R CrB stars is explained by invoking mixing between the C-O WD which contains C but no N, and the He WD which contains N but no C. The mixing takes place possibly at the time of merging (Iben & Tutukov 1985). Asplund et al. (2000) speculate that the *rp*-process, primarily α-particle capture, might synthesize the intermediate-mass elements Na−S, and so account for the unusual Si/Fe and S/Fe ratios of minority R CrB stars. Detailed calculations of the nucleosynthesis expected from a merger have not been reported. Saio & Jeffery (2000) have examined the evolution of two merged He white dwarfs and could explain the observed properties of low-luminosity (or high-gravity) EHes, in particular of V652 Her, with its low C/He ratio.

An important fact about the compositions of the EHes and the R CrB stars is that the O abundances are on average the 'normal' values (i.e., [O/M] is approximately centred on 0), and the maximum N abundances are consistent with conversion of the initial C and O, as judged by the metallicity [M] (derived from the mean of Si and S), to N by the CNO-cycles. In the DD scenario, these facts must emerge from details of the merging process. The following simple picture of a merger of a He white dwarf with a C−O white dwarf attempts to illustrate this point.

The He white dwarf contains primarily He with N, the principal product of H-burning, as the second most abundant element but is not enriched in *s*-process elements. A thin skin of H completes the structure. The C−O white dwarf may contain a thin shell which was part of the He-shell of the AGB star. This shell will contain He, C and O, and is probably enriched in the *s*-process heavy elements. Below this shell, the bulk of the white dwarf will be C and O. It is worth noting that this scenario probably accounts for the absence of *s*-process enrichment in the EHes and R CrB stars; the He white dwarf will not have been exposed to a neutron source, and while the surface of the C−O white dwarf may be *s*-process enriched having been the core of an AGB star, little material from this star is needed to account for the C/He ratio of our stars. Merging may resemble the mixing of our simple recipe. Nitrogen is provided by the accreted material from the He white dwarf, and provided that this material dominates the atmosphere of the merged star, the N abundance will approach that expected from conversion of initial C and O to N. The C/He ratio is determined by the mixing of the accreted material (He) with the outer layers of the C−O white dwarf (a mixture of He, C and O). With mass fractions of unity for He in the accreted material and, perhaps, about 0.2 for the C−O material, it is clear that only if the accreted material dominates the merged star can the observed low C/He ratios be obtained. Similarly, a low O/M ratio is achieved only if the accreted material dominates. Our rough calculation suggests that a 10 to 1 mix of the He white dwarf to the C−O white dwarf produces a merged star with a composition similar to the observed compositions. Theoretical calculations have yet to determine the mixing fraction, and the range that it may assume. Our assumption of quiescent merging is possibly incorrect. Accretion of material may ignite a carbon-oxygen shell. Thermal flashes and mixing may ensue. Such flashes in the C−O white dwarf were considered by Saio &

Nomoto (1998), and by Saio & Jeffery (2000) considering accretion of He-rich material by a He white dwarf. The presence of freshly synthesized material in the merged star enhances the coincidence that the composition matches the 'normal' O/M of the observed stars.

In Saio & Jeffery's (2000) calculations, the accreted He-rich material was presumed to come from a second white dwarf in a merger. This model was devised to account for V652 Her, the hot pulsating EHe with the low C/He ratio. Emphasis was placed not on matching the observed chemical composition, but on fitting the pulsations and their time derivative. He-shell flashes occur in the star allowing for some C to be mixed to the surface following the first flash. Since V652 Her has the composition of a He-rich layer that results from CNO-cycling, the merged star replicates the observed composition. Constraints on mergers of He with C−O white dwarfs are more severe with some elements provided primarily by the accreted material, others by the C−O white dwarf, with some elements dependent on the nucleosynthesis in the flashes and the mixing between the flashed material and the envelope; calculations are awaited with interest.

In summary, the FF scenario cannot account for the typical EHe and R CrB star. The DD scenario remains a possible explanation, but perhaps only until detailed calculations are reported! The existence of minority R CrB stars with spectacular Si/Fe and S/Fe ratios may be an indication of yet another scenario.

10 CONCLUSIONS

Our sample of cool EHes shows that their compositions resemble in many ways those of hot EHes and the R CrB stars; they might be termed transition objects between these two groups of He-rich stars. Close inspection of the analysed EHes – hot and cool – and the R CrB stars – majority and minority – show a significant difference in the N abundances. If the initial metallicity of a star is assessed from its present Si and S abundances, the N abundance of majority R CrB stars implies full conversion of initial C and O to N by the CNO-cycles. EHes show generally lower N abundances, with several exhibiting only mild N enrichment. This mildness appears misleading because N provided by conversion of the initial C and O to N may have been processed by α-captures to ^{22}Ne; there is evidence for this neon in several stars. Their different N abundances could suggest that the R CrB stars and EHes are not on the same evolutionary path, although their formation may be triggered by similar events. Alternatively, the higher N abundance of the R CrB stars resulted when EHes evolved to red giants and a little C was processed by the residual H to N.

A majority of the stars show evidence of three components in their atmosphere: a residue of normal H-rich material, substantial amounts of H-poor CN(O)-cycled material, and C- (and O-) rich material from gas exposed to He-burning. This combination could be provided by a single star, as in the FF scenario, or by a merger of white dwarfs, as in the DD scenario. Although the FF scenario accounts for Sakurai's object and other stars (e.g., the H-poor central stars of planetary nebulae), present simulations imply much higher C/He and O/He ratios than are observed in EHes and R CrB stars. The observed abundances imply constraints on the merger process and subsequent evolution of the merged He-rich star that results from the DD scenario and merger of a He white dwarf with either a C−O or a He white dwarf. Theoretical evaluations of the DD scenario have yet to grapple with these constraints. There remains too the intriguing problem of the minority R CrB stars and similar stars with extraordinary ratios of Si/Fe and S/Fe, for

example. Is there a nuclear origin for these anomalies? Or are they the result of a winnowing of dust from gas?

Although an observer's lament of 'more observations' applies – for example, measurements of Ne and Mg in R CrB stars are of interest; also, the *s*-process elements in EHes are crucial to see whether $^{22}Ne(\alpha, n)^{25}Mg$ can be a neutron source – the louder plea might be for additional theoretical work on the FF and, especially, on the DD scenario. Additionally, it should not be assumed that the origins of EHes and R CrB stars are to be found in the DD or FF scenarios.

Finally, it is surely of interest that H in these He-rich stars, with the exception of the two EHes with a low C/He ratio, is depleted by at least 3 dex. This raises the question – why are there no mildly H-poor relatives of the EHes in the same temperature range? To which an answer may be – there are, but they are difficult to identify. In support of this notion, we note that, in the case of the R CrB stars that are more easily betrayed by their distinctive declines, H has been detected with an abundance 2 dex greater than in the most H-rich EHe where H is depleted by just a factor of 1.3 dex. An alternative answer may be that conversion of a H-rich to a He-rich star is almost always so complete that mildly H-poor stars do not exist, or exist for only a very short time. Discovery of mildly H-poor relatives of the EHes and also additional R CrB stars would be of great interest. Certainly, at effective temperatures of the EHes and hotter, there are stars of intermediate H-deficiency. At the highest temperatures, the H abundance is difficult to determine from optical spectra. One may expect that mild cases of H deficiency arise for reasons unrelated to the origins of the EHes and R CrB stars.

ACKNOWLEDGMENTS

REFERENCES

Arnould M., Goriely S., Jorissen A., 1999, A&A, 347, 572
Asplund M., 2000, Oxygen Abundances in Old Stars and Implications to Nucleosynthesis and Cosmology, 24th meeting of the IAU, Joint Discussion 8, August 2000. Manchester, England
Asplund M., García Pérez A. E., 2001, A&A, accepted
Asplund M., Gustafsson B., Kiselman D., Eriksson K., 1997a, A&A, 318, 521
Asplund M., Gustafsson B., Lambert D. L., Rao N. K., 1997b, A&A, 321, L17
Asplund M., Gustafsson B., Rao N. K., Lambert D. L., 1998, A&A, 332, 651
Asplund M., Lambert D. L., Kipper T., Pollacco D., Shetrone M. D., 1999, A&A, 343, 507
Asplund M., Gustafsson B., Lambert D. L., Rao N. K., 2000, A&A, 353, 287
Auer L. H., Mihalas D., 1973, ApJ, 184, 151
Bassalo J. M., Cattani M., Walder V. S., 1980, Phys. Rev. A, 22, 1194
Boesgaard A. M., King J. R., Deliyannis C. P., Vogt S. S., 1999, AJ, 117, 492
Caloi V., 1989, A&A, 221, 27
Carretta E., Gratton R. G., Sneden C., 2000, A&A, 356, 238
Chiba M., Yoshii Y., 1998, AJ, 115, 168
Dimitrijevic M. S., Sahal-Bréchot S., 1984, J. Quant. Spectrosc. Radiat. Transfer, 31, 301
Dreizler S., 1999, A&A, 352, 632
Dreizler S., Heber U., 1998, A&A, 334, 618

Drilling J. S., 1979, ApJ, 228, 491
Drilling J. S., 1980, ApJ, 242, L43
Drilling J. S., Jeffery C. S., Heber U., 1998, A&A, 329, 1019
Fujimoto M. Y., 1977, PASJ, 29, 331
Giridhar S., Lambert D. L., Gonzalez G., 2000, ApJ, 531, 521
Goswami A., Prantzos N., 2000, A&A, 359, 191
Grevesse N., Noels A., Sauval A. J., 1996, in Holt S. S., Sonneborn G., eds, ASP Conf. Ser. Vol. 99, Cosmic Abundances. Astron. Soc. Pac., San Francisco, p. 117
Griem H. R., Baranger M., Kolb A. C., Oertel G., 1962, Phys. Rev., 125, 177
Haas S., Dreizler S., Heber U., Jeffery S., Werner K., 1996, A&A, 311, 669
Harrison P. M., Jeffery C. S., 1997, A&A, 323, 177
Heber U., 1983, A&A, 118, 39
Heber U., Schönberner D., 1981, A&A, 102, 73
Herwig F., 2001, Ap&SS, 275, 15
Herwig F., 2000, A&A, 360, 952
Herwig F., Blöcker T., Driebe T., 1999, A&A, 349, L5
Hibbert A., Biémont E., Godefroid M., Vaeck N., 1993, A&AS, 99, 179
Hill P. W., 1964, MNRAS, 127, 113
Hill P. W., 1965, MNRAS, 129, 137
Hunger K., 1975, in Baschek B., Kegel W. H., Traving G., eds, Problems in Stellar Atmospheres and Envelopes. Springer-Verlag, New York, p. 57
Husfeld D., Butler K., Heber U., Drilling J. S., 1989, A&A, 222, 150
Iben I., Jr, Renzini A., 1983, ARA&A, 21, 271
Iben I., Jr, Tutukov A. V., 1985, ApJS, 58, 661
Iben I., Jr, Tutukov A. V., Yungelson L. R., 1996, ApJ, 456, 750
Israelian G., García López R. J., Rebolo R., 1998, ApJ, 507, 805
Israelian G., Rebolo R., Basri G., Casares J., Martin E. L., 1999, Nat, 401, 142
Jeffery C. S., 1994, CCP7 Newsletter on 'The Analysis of Astronomical Spectra', No. 16, p. 17
Jeffery C. S., 1996, in Jeffery C. S., Heber U., eds, ASP Conf. Ser. Vol. 96, Hydrogen deficient stars. Astron. Soc. Pac., San Francisco, p. 152
Jeffery C. S., 1998, MNRAS, 294, 391
Jeffery C. S., Harrison P. M., 1997, A&A, 323, 393
Jeffery C. S., Heber U., 1992, A&A, 260, 133
Jeffery C. S., Heber U., 1993, A&A, 270, 167
Jeffery C. S., Drilling J. S., Heber U., 1987, MNRAS, 226, 317
Jeffery C. S., Heber U., Hill P. W., Dreizler S., Drilling J. S., Lawson W. A., Leuenhagen U., Werner K., 1996, in Jeffery C. S., Heber U., eds, ASP Conf. Ser. Vol. 96, Hydrogen Deficient Stars. Astron. Soc. Pac., San Francisco, p. 471
Jeffery C. S., Hamill P. J., Harrison P. M., Jeffers S. V., 1998, A&A, 340, 476
Jeffery C. S., Hill P. W., Heber U., 1999, A&A, 346, 491
Kelleher D. E., 1981, J. Quant. Spectrosc. Radiat. Transfer, 25, 191
King J. R., 2000, AJ, 120, 1056
Kurucz R. L., Peytremann E., 1975, SAO – Special Report No. 362
Lambert D. L., 1989, Cosmic Abundances of Matter; Proceedings of the AIP Conference, Minneapolis, MN, September 7–9, 1988 (A90-31833 13-90). American Institute of Physics, New York, p. 168
Lambert D. L., 2000, Oxygen Abundances in Old Stars and Implications to Nucleosynthesis and Cosmology, 24th meeting of the IAU, Joint Discussion 8, August 2000. Manchester, England
Lambert D. L., Rao N. K., 1994, JA&A, 15, 47
Leuenhagen U., Hamann W.-R., 1998, A&A, 330, 265
Luo D., Pradhan A. K., 1989, J. Phys. B., 22, 3377
Lynas-Gray A. E., Walker H. J., Hill P. W., Kaufmann J. P., 1981, A&AS, 44, 349
Moore Ch. E., 1970, Selected Tables of Atomic Spectra, Sect. 3 (C I–IV). NBS, Washington
Moore Ch. E., 1972, A Multiplet Table of Astrophysical Interest. NSRDS – NBS 40, Washington
Nissen P. E., Primas F., Asplund M., 2000, Oxygen Abundances in Old Stars and Implications to Nucleosynthesis and Cosmology, 24th meeting of the IAU, Joint Discussion 8, August 2000. Manchester, England

Odintsov V. I., 1965, Opt. Spectrosc., 18, 205

Pandey G., 1999, PhD thesis, Univ. Bangalore

Pandey G., Rao N. K., Lambert D. L., 1996, MNRAS, 282, 889

Peach G., 1970, MemRAS, 73, 1

Popper D. M., 1942, PASP, 54, 160

Rao N. K., Lambert D. L., 1996, in Jeffery C. S., Heber U., eds, ASP Conf. Ser. Vol. 96, Hydrogen Deficient Stars. Astron. Soc. Pac., San Francisco, p. 152

Rao N. K. et al., 1999, MNRAS, 310, 717

Rauch T., Köppen J., Werner K., 1994, A&A, 286, 543

Saio H., Jeffery C. S., 2000, MNRAS, 313, 671

Saio H., Nomoto K., 1998, ApJ, 500, 388

Schönberner D., 1975, A&A, 44, 383

Schönberner D., 1979, A&A, 79, 108

Schönberner D., 1983, ApJ, 272, 708

Schönberner D., 1996, in Jeffery C. S., Heber U., eds, ASP Conf. Ser. Vol. 96, Hydrogen Deficient Stars. Astron. Soc. Pac., San Francisco, p. 433

Schönberner D., Wolf R. E. A., 1974, A&A, 37, 87

Seaton M. J., Yan Y., Mihalas D., Pradhan A. K., 1994, MNRAS, 266, 805

Thackeray A. D., Wesselink A. J., 1952, Observatory, 72, 248

Thévenin F., 1989, A&AS, 77, 137

Thévenin F., 1990, A&AS, 82, 179

Tull R. G., MacQueen P. J., Sneden C., Lambert D. L., 1995, PASP, 107, 251

Van Winckel H., Waelkens C., Waters L. B. F. M., 1995, A&A, 293, L25

Walker H. J., Schönberner D., 1981, A&A, 97, 291

Warner B., 1967, MNRAS, 137, 119

Webbink R. F., 1984, ApJ, 277, 355

Wheeler J. C., Sneden C., Truran J., 1989, ARA&A, 27, 279

Wiese W. L., Smith M. W., Glennon B. M., 1966, National Bureau of Standards (USA) Publs. Vols I–II, Atomic Transition Probabilities. NBS, Washington

APPENDIX A: ERROR ANALYSIS

The major sources of error in deriving the abundances are the line-to-line scatter of the abundances, and uncertainty in the adopted stellar parameters. The stellar parameters are accurate to typically: $\Delta T_{\rm eff} = \pm 300$ K, $\Delta \log g = \pm 0.5$ [cgs] and $\Delta \xi = \pm 1$ km s^{-1}. The derivatives of mean ion abundances with respect to $T_{\rm eff}$ and $\log g$ were calculated. The maximum error in each ion abundance is estimated. For the majority of the ions, these errors are smaller than the line-to-line scatter (standard deviation due to several lines belonging to the same ion). The mean maximum error in the derived abundances corresponding to the uncertainty in $T_{\rm eff}$ and $\log g$ is about 0.1 dex; the errors due to the uncertainty in ξ are negligible when compared to that due to uncertainties in the other parameters.

The mean abundance of an element X, was calculated as

$$\langle X \rangle = \frac{w_1 \langle XI \rangle + w_2 \langle XII \rangle + \ldots}{w_1 + w_2 + \ldots},$$

Table A1. SAMPLE, the full line lists are present as Supplementary Material in the electronic version of the journal, available on *Synergy*.

Ion λ (Å)	χ (eV)	$\log gf$	W_λ (mÅ)	$\log \epsilon$ [a]	Ref.[b]
H I						
6562.80	10.2	0.71	515	6.30	Luck
He I						
3871.82	21.13	−1.92	Synth[c]	11.54	Jeffery
5047.74	14.06	−0.62	Synth	11.54	Jeffery
C I						
4371.33	7.68	−1.96	261	9.39	OP
4734.26	7.95	−2.37	191	9.36	OP

where $\langle XI \rangle$, $\langle XII \rangle$, ... are the abundance of element X derived from neutral, singly ionized, ... lines of element X. $w_1, w_2, \ldots$ are weights, i.e.,

$$w_1 = \frac{1}{(\delta \langle XI \rangle)^2}.$$

$\delta \langle XI \rangle$ is the error in $\langle XI \rangle$ due to the uncertainty in $T_{\rm eff}$ and $\log g$.

The error in the ratio say X/Fe was calculated as

$$\delta(X/Fe) = \frac{(\delta \langle X \rangle) \langle Fe \rangle - (\delta \langle Fe \rangle) \langle X \rangle}{\langle Fe \rangle^2},$$

where

$$(\delta \langle X \rangle)^2 = \frac{1}{w_1 + w_2 + \ldots}.$$

We take the modulus of

$$\frac{(\delta \langle X \rangle) \langle Fe \rangle - (\delta \langle Fe \rangle) \langle X \rangle}{\langle Fe \rangle^2}$$

to estimate the error in X/Fe.

Abundance ratios are generally less affected by these uncertainties, because most elements are sensitive to the stellar parameters in the same way.

The final abundances derived from neutral and ionized species of an element are separately given in Table 2 for our programme stars. The hydrogen abundance is determined from the measured equivalent width of the Hα line.

This paper has been typeset from a TeX/LaTeX file prepared by the author.